

Agrobacterium-delivered VirE2 interacts with host nucleoporin CG1 to facilitate the nuclear import of VirE2-coated T complex

Xiaoyang Li^a, Qinghua Yang^{a,1}, Ling Peng^{a,1}, Haitao Tu^b, Lan-Ying Lee^c, Stanton B. Gelvin^c, and Shen Q. Pan^{a,2}

^aDepartment of Biological Sciences, National University of Singapore, Singapore 117543; ^bSchool of Stomatology and Medicine, Foshan University, Foshan 528000, China; and ^cDepartment of Biological Sciences, Purdue University, West Lafayette, IN 47907

Edited by Mark Estelle, University of California San Diego, La Jolla, CA, and approved September 9, 2020 (received for review May 15, 2020)

Agrobacterium tumefaciens is the causal agent of crown gall disease. The bacterium is capable of transferring a segment of single-stranded DNA (ssDNA) into recipient cells during the transformation process, and it has been widely used as a genetic modification tool for plants and nonplant organisms. Transferred DNA (T-DNA) has been proposed to be escorted by two virulence proteins, VirD2 and VirE2, as a nucleoprotein complex (T-complex) that targets the host nucleus. However, it is not clear how such a proposed large DNA-protein complex is delivered through the host nuclear pore in a natural setting. Here, we studied the natural nuclear import of the *Agrobacterium*-delivered ssDNA-binding protein VirE2 inside plant cells by using a split-GFP approach with a newly constructed T-DNA-free strain. Our results demonstrate that VirE2 is targeted into the host nucleus in a VirD2- and T-DNA-dependent manner. In contrast with VirD2 that binds to plant importin α for nuclear import, VirE2 directly interacts with the host nuclear pore complex component nucleoporin CG1 to facilitate its nuclear uptake and the transformation process. Our data suggest a cooperative nuclear import model in which T-DNA is guided to the host nuclear pore by VirD2 and passes through the pore with the assistance of interactions between VirE2 and host nucleoporin CG1. We hypothesize that this large linear nucleoprotein complex (T-complex) is targeted to the nucleus by a “head” guide from the VirD2–importin interaction and into the nucleus by a lateral assistance from the VirE2–nucleoporin interaction.

Agrobacterium | VirE2 | T-complex | CG1 | nuclear import

As a natural genetic engineer, *Agrobacterium tumefaciens* processes a segment of DNA, transferred DNA (T-DNA), from the bacterial Ti plasmid and delivers it into host cells (1, 2). T-DNA is delivered as single-stranded DNA (ssDNA) into the host nucleus and may be integrated into the host genome (3). The expression of oncogenic genes residing on T-DNA causes crown gall tumors on host plants. Under laboratory conditions, *Agrobacterium* can also deliver T-DNA into yeast (4, 5), nonyeast fungal (6), and algal cells (7). This unique ability has enabled the use of this bacterium as an important tool for genetically transforming plant and fungal cells (8, 9).

The T-DNA region is located on a bacterial tumor-inducing (Ti) plasmid and is delineated by specific border sequences (10). At the initial stage of *Agrobacterium*-mediated transformation (AMT), the virulence protein VirD2 nicks the T-DNA borders and releases T-DNA from the Ti plasmid to generate an ssDNA fragment (11, 12). The 5′ end of T-DNA remains covalently attached to VirD2 and is delivered into the host cell through a type IV secretion system (T4SS) (13, 14). Inside host cells, T-DNA is hypothesized to be further coated by the virulence protein VirE2, which is also delivered through the T4SS, to form the T-complex (15–17). VirE2 is an ssDNA-binding protein that can protect T-DNA from nucleolytic degradation and facilitate its transport in the host cell (18–21). Assembly of the T-complex is proposed to occur at the host cell entrance where VirE3

facilitates the assembly of a VirE2-coated T-complex (22), which is then targeted to the host nucleus.

Nuclear targeting of the T-complex is proposed to be mediated by VirD2 and VirE2. Various studies have observed differences between the nuclear import of VirD2 and VirE2 in plants and nonplant cells (23). In eukaryotic cells, active import of proteins into nuclei is mainly mediated by a group of nuclear transport receptors (NTRs) which recognize the cargo through specific sequences called nuclear localization signal (NLS) sequences (24, 25). Previous studies have shown that VirD2 localized to the nucleus of plants and nonplant organisms, indicating the presence of evolutionarily conserved NLS(s) in VirD2 (23). Indeed, an N-terminal monopartite NLS and two C-terminal bipartite NLSs have been identified in VirD2 (26–28), and the two C-terminal NLSs were further shown to be functional and important for the transformation process (27, 29). Moreover, interaction of VirD2 with plant importin α suggests that the canonical importin-dependent pathway is involved in the nuclear import of VirD2 in host cells (30, 31).

In contrast, the nuclear uptake of VirE2 remains controversial. VirE2 was reported to target nuclei of plant cells but not nonplant species, indicating that the nuclear import of VirE2 may be plant-specific (32). However, conflicting results were also reported for the nuclear import of VirE2 in plant cells. Several reports demonstrated that VirE2 could localize to the plant nucleus, while others only observed cytoplasmic localization (33). Although the

Significance

Molecular trafficking into nuclei is essential for eukaryotic cells. However, it is not clear how a large linear protein complex enters the nucleus in a natural setting. *Agrobacterium* delivers T-DNA along with the protein VirD2 and perhaps VirE2 into the host nucleus. Here, we report that VirD2 provides the guide on the “head” and VirE2 provides the lateral assistance to facilitate nuclear import of the T-DNA–protein complex. VirE2 directly interacts with the host nuclear pore complex component nucleoporin CG1 to facilitate nuclear uptake of the T-complex and the transformation process. Our findings shed light on how a pathogen delivers large linear nucleoprotein complexes into host nuclei.

Author contributions: X.L. and S.Q.P. designed research; X.L., Q.Y., L.P., H.T., and L.-Y.L. performed research; X.L., S.B.G., and S.Q.P. analyzed data; X.L., S.B.G., and S.Q.P. wrote the paper; and S.Q.P. supervised the project.

The authors declare no competing interest.

This article is a PNAS Direct Submission.

Published under the PNAS license.

¹Present address: School of Basic Medicine, Guizhou University of Traditional Chinese Medicine, Guiyang 550025, China.

²To whom correspondence may be addressed. Email: dbspansq@nus.edu.sg.

This article contains supporting information online at <https://www.pnas.org/lookup/suppl/doi:10.1073/pnas.2009645117/-DCSupplemental>.

First published October 5, 2020.

existence of two potential NLSs in VirE2 has been proposed (34), VirE2 expressed alone remained in the host cytoplasm (33) and the association of VirE2 with importin α was weak and likely nonphysiological (35), indicating that the two putative NLSs might not be functional *in vivo*. Moreover, two additional proteins, VIP1 and VirE3, were reported to facilitate nuclear uptake of VirE2 in host cells (36, 37). However, more recent studies indicated that VIP1 is not important for the AMT process (38, 39), whereas VirE3 may be involved in T-complex assembly and does not localize to the plant nucleus (22, 40). Thus, it is not clear whether and how VirE2 is imported into the host nucleus.

Nuclear import of the T-complex was proposed to occur in a polar fashion, with VirD2 functioning as the pilot during transport. Although both VirD2 and VirE2 are needed for efficient nuclear import of T-DNA in permeabilized cells (41), it remains unknown how the process is coordinated and what host factors are involved in the directional import of the proposed T-complex into host nuclei in a natural setting.

In this study, we found that VirE2 directly interacts with the host nuclear pore complex component nucleoporin CG1, which was found to be important for VirE2 nuclear import and the transformation process. The VirE2–CG1 interaction did not involve the previously identified NLS of VirE2. Our data suggest that the T-complex is transported into the host nucleus in a cooperative manner, where VirD2 provides the guide on the “head” through its NLS-mediated interaction with plant importin α , whereas VirE2 provides the assistance on the lateral side of the T-complex via VirE2–CG1 interaction to facilitate the nuclear import of T-DNA.

Results

Both VirD2 and T-DNA Are Required for Import of VirE2 into the Plant Nucleus. To track *Agrobacterium*-delivered VirE2 inside the host cell, a split-GFP based approach was adopted as previously described (42, 43). Briefly, the β -strand 11 of GFP (GFP11) was used to label VirE2 and expressed as VirE2-GFP11 inside bacterial cells, whereas the β -strands 1–10 of GFP was expressed as GFP1–10 inside host cells; spontaneous complementation occurs upon VirE2-GFP11 translocation and leads to a green fluorescence signal VirE2-GFP_{comp} in the host cells. We previously showed that VirE2-GFP11 functions similarly to wild-type VirE2 (42); therefore, VirE2-GFP_{comp} can be used to study the trafficking of *Agrobacterium*-delivered VirE2 inside plant cells that express GFP1–10 in a natural setting.

To study *Agrobacterium*-delivered VirE2 in plant cells, *A. tumefaciens* strain EHA105 was used initially in this study; this strain is widely used for plant transformation because it contains a disarmed Ti plasmid (pTiEHA105), which was constructed by removing the oncogenic T-DNA region from the Ti plasmid pTiBo542 (44). To visualize *Agrobacterium*-delivered VirE2 in plant cells, GFP11 was used to label VirE2 in *A. tumefaciens* EHA105 as described (42); the GFP11-tagged strain EHA105virE2::GFP11 expressing VirE2-GFP11 was infiltrated into the leaves of transgenic *Nicotiana benthamiana* plants (Nb308A) expressing both GFP1–10 and DsRed. DsRed expression in *N. benthamiana* leaf epidermal cells facilitated the visualization of the cellular borders and the nuclei, which are mostly round or oval (Fig. 1). VirE2 delivered from *Agrobacterium* was visualized in *N. benthamiana* leaf epidermal cells using confocal microscopy 2 d post-agroinfiltration (Fig. 1A). As shown in Fig. 1A, Upper, when an *Agrobacterium* strain containing VirD2 and a T-DNA was used for infection, a portion of VirE2 could be detected inside the host nucleus, although the majority of VirE2 stayed in the host cytoplasm. To investigate the roles played by different effectors on VirE2 trafficking and localization, individual deletion mutants for the known effectors (VirD2, VirD5, VirE3, and VirF) were generated. The corresponding mutants expressing VirE2-GFP11 were then infiltrated into *N. benthamiana* Nb308A leaves

followed by VirE2 visualization. Interestingly, deletion of *virD2* dramatically affected the distribution of VirE2 inside the host cell; no obvious nuclear accumulation of VirE2 could be observed (Fig. 1A and B). The *virD2* deletion was nonpolar and did not compromise the function of the downstream gene *virD4*, as VirE2 secretion from the mutant into host cells was not affected (Fig. 1A and SI Appendix, Fig. S1). In contrast, deletion of other virulence effector protein genes (*virD5*, *virE3*, and *virF*) did not affect the nuclear import of VirE2 significantly (SI Appendix, Fig. S1). Moreover, transiently expressed VirE2-cYFP and VirE2-nYFP could not localize to the nucleus of tobacco BY-2 protoplasts in a bimolecular fluorescence complementation experiment (SI Appendix, Fig. S2A), indicating that VirE2 alone is not able to target the nucleus of plant cells. Finally, small amounts of VirE2-Venus could localize to nuclei of agroinfiltrated *N. benthamiana* epidermal cells, confirming that when VirE2 is made *in planta* in the presence of VirD2 and T-DNA, nuclear localization could occur (SI Appendix, Fig. S2B).

VirE2 is hypothesized to coat T-DNA attached to VirD2 to form the T-complex upon delivery; thus, these molecules may move together inside host cells. To examine the role of T-DNA in VirE2 nuclear import, a T-DNA-free strain is needed. *A. tumefaciens* EHA105 has been considered to be T-DNA free, as the oncogenic T-DNA region was deleted (44). However, a T-DNA left border was still left on the Ti plasmid pTiEHA105 (44). Previous studies suggested that T-DNA could be initiated through the left border (45), indicating that T-DNA might still be generated inside the *A. tumefaciens* strain EHA105. To investigate whether the potential T-DNA would affect the nuclear import of VirE2, we deleted the T-DNA left border from the Ti plasmid of *A. tumefaciens* EHA105virE2::GFP11 and generated XYA105virE2::GFP11 (SI Appendix, Fig. S3). As shown in Fig. 1C, Upper, deletion of the T-DNA left border abolished the nuclear accumulation of VirE2 in *N. benthamiana* leaf epidermal cells, indicating that nuclear import of VirE2 in plant cells is dependent on the presence of T-DNA. Moreover, introducing a T-DNA binary plasmid (pXY01) into the T-DNA-free strain XYA105virE2::GFP11 restored VirE2 accumulation inside host nuclei (Fig. 1C and D). To confirm the roles of VirD2 and T-DNA in the nuclear import of VirE2, a transgenic *N. benthamiana* line (Nb308E2) expressing VirE2-GFP11, GFP1–10, and DsRed was generated. VirE2-GFP_{comp} expressed in plant cells alone was restricted to the plant cytoplasm; and the expressed VirE2-GFP_{comp} could relocate to the host nucleus in the presence of both VirD2 and T-DNA (SI Appendix, Fig. S2 C and D). Taken together, these results suggest that both VirD2 and T-DNA are required for the nuclear import of VirE2, and VirE2 can only enter the plant nucleus as a T-complex component.

The Two Putative NLSs of VirE2 Do Not Function in Plant Cells. The nucleus in a eukaryotic cell is surrounded by the nuclear envelope, which is made up of two lipid bilayer membranes. Transport of molecules across the nuclear envelope occurs predominantly through the nuclear pore complex (NPC) (46, 47). NPCs allow the passive diffusion of small molecules, including proteins with a molecular mass below ~40 kDa (48). As the sizes of both VirE2 and VirD2 exceed the passive diffusion limit, active transport mechanisms are required for the import of these two virulence proteins into the host nucleus.

Active import of large protein molecules into the nucleus is mediated by NTRs, most of which belong to the karyopherin protein family (49). Among the NTRs, importin α recognizes cargos through specific NLSs and functions as an adaptor protein between the cargo and importin β , which ferries the protein complex across the NPC (24, 25). Two putative NLSs have been identified in VirE2 (SI Appendix, Fig. S4A) (34). To test whether the two putative NLSs of VirE2 are functional, we investigated the interactions between VirE2 and plant importin α isoforms. Nine importin α isoforms have been identified in *Arabidopsis*

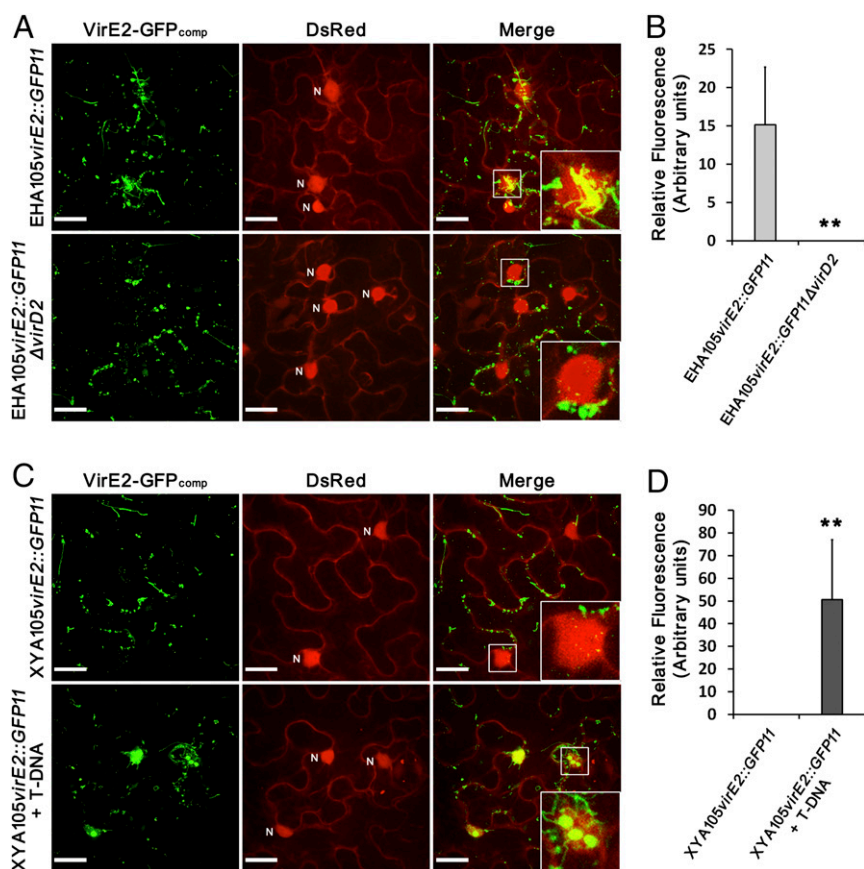


Fig. 1. Both VirD2 and T-DNA are required for the import of VirE2 into the plant nucleus. (A) VirD2 is required for the nuclear import of VirE2 in plant cells. Transgenic *N. benthamiana* (Nb308A) (expressing both GFP10 and DsRed) leaves were infiltrated with *A. tumefaciens* strains EHA105virE2::GFP11 (Upper) or EHA105virE2::GFP11ΔvirD2 (Lower). (B) The fluorescence intensity of VirE2-GFP_{comp} signals was measured in each host nucleus. The data are presented as the means \pm SD of $n = 30$ independent samples. (C) T-DNA is required for the nuclear import of VirE2 in plant cells. Transgenic *N. benthamiana* (Nb308A) leaves were infiltrated with *A. tumefaciens* strains XYA105virE2::GFP11 (Upper) or XYA105virE2::GFP11 containing a binary plasmid pXY01 (Lower). (D) The fluorescence intensity of VirE2-GFP_{comp} signals was measured in each host nucleus. The data are presented as the means \pm SD of $n = 30$ independent samples. DsRed expression in *N. benthamiana* leaf epidermal cells facilitated the visualization of the cellular borders and the round/oval nuclei (N). The boxed areas are enlarged to highlight host nuclei. (Scale bars, 20 μ m.) ** $P < 0.01$.

thaliana (31). A yeast two-hybrid approach was used to examine the interactions between VirE2 and each of these nine importin α isoforms. In these assays, the importin α isoforms were expressed as translational fusions to the GAL4 activation domain (AD) and VirE2 was expressed as a translational fusion to the GAL4 DNA-binding domain (BD). As shown in Fig. 2A, we could not detect any interaction between VirE2 and the tested importin α isoforms in the yeast two-hybrid assays. To confirm further these results, we performed in vitro pull-down assays using GST-fused importin α isoforms as the baits and VirE2 as the prey. As shown in Fig. 2B, we could not coprecipitate VirE2 with any of the nine GST-fused importin α isoforms, indicating that VirE2 might not show strong interactions with plant importin α .

In contrast, we observed interactions between VirD2 and several *A. thaliana* importin α isoforms under these same conditions. As shown in Fig. 2C, yeast two-hybrid assay results revealed that VirD2 could interact with six of the nine importin α isoforms, but not with IMPA-5, IMPA-8, and IMPA-9. The interactions were further confirmed by GST pull-down assays (Fig. 2D). These results suggest that VirD2 can interact with some plant importin α proteins and presumably utilizes the importin-dependent pathway for nuclear import.

The two putative NLSs of VirE2 are located in the middle of the protein (SI Appendix, Fig. S4A); potentially, they might be

structurally covered after protein folding. To investigate further whether the two putative NLSs are functional in plant cells, we transiently expressed these two regions as translational fusions to a tandem mCherry_{x4} reporter in *N. benthamiana* leaf epidermal cells. The 4 \times mCherry was used to increase the size of the fluorescent protein tag to restrict its presence to the cytoplasm so that the potential nuclear localization may be studied. As shown in Fig. 2E, transiently expressed mCherry_{x4} alone was restricted to the cytoplasm of the plant cells, whereas mCherry_{x4} fused to a C-terminal NLS of VirD2 or an NLS from simian virus 40 (SV40) could target the plant nucleus efficiently. These results indicate that VirD2 contains an NLS that is functional inside the plant cell (SI Appendix, Fig. S4B and Fig. 2E). In contrast, mCherry_{x4} fused to either of the two putative NLS regions of VirE2 was not imported into the plant nucleus, suggesting that these two regions of VirE2 could not function as NLS in plant cells (Fig. 2E).

Taken together, our results suggest that VirE2, unlike VirD2, may not contain a strong NLS that can function with plant importin α in plant cells. VirE2 may exploit an importin-independent pathway for its nuclear transportation.

VirE2 Interacts with Host NPC Component Nucleoporin CG1. NPCs act as physical barriers that keep the nucleus from freely exchanging with the cytoplasm. For import into the nucleus, protein cargos

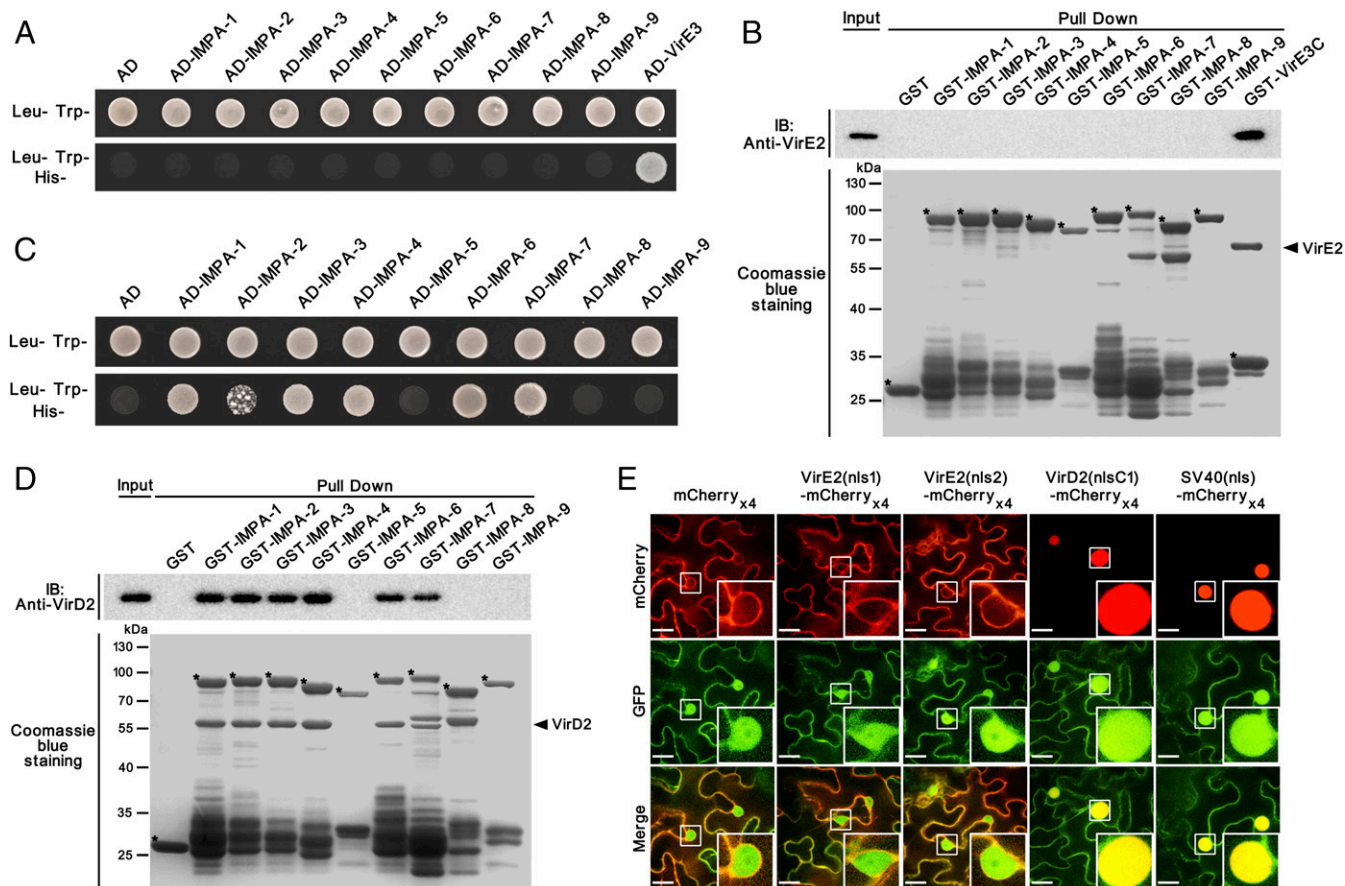


Fig. 2. The two putative NLSs of VirE2 do not function in plant cells. (A) VirE2 does not interact with any of the nine importin α isoforms from *A. thaliana* in the yeast two-hybrid assays. The importin α isoforms were expressed as translational fusions to the GAL4 AD, and VirE2 was expressed as a translational fusion to the GAL4 BD. Interaction of BD-VirE2 with AD-VirE3 served as a positive control; (B) VirE2 does not interact with any of the nine importin α isoforms from *A. thaliana* in GST pull-down assays. Importin α isoforms fused to GST were used as the baits, and VirE2 was used as the prey in pull-down assays. The GST-fused VirE2-interacting domain from VirE3 was used as a positive control. The pull-down fractions and 10% of the input were analyzed by Western blots (Upper). The pull-down fractions were visualized with Coomassie blue stain (Lower); GST-fused baits are indicated by asterisks. IB, immunoblot. (C) VirD2 interacts with six of the nine *A. thaliana* importin α isoforms in the yeast two-hybrid assays. The importin α isoforms were expressed as translational fusions to the GAL4 AD, and VirD2 was expressed as a translational fusion to the GAL4 BD. (D) VirD2 interacts with six of the nine *A. thaliana* importin α isoforms in the GST pull-down assays. Importin α isoforms fused to GST were used as the baits and VirD2 was used as the prey in the pull-down assays. The pull-down fractions and 10% of the input were analyzed by Western blot (Upper). The pull-down fractions were visualized with Coomassie blue stain (Lower), and GST-fused baits were indicated by asterisks. (E) The two putative NLS regions of VirE2 could not function as an NLS in plant cells. Wild-type *N. benthamiana* leaves were infiltrated with equal quantities of *A. tumefaciens* XYA105 containing the binary plasmid pXY01-GFP, and XYA105 containing the binary plasmids expressing mCherry_{x4}-labeled peptides from VirE2 and VirD2. mCherry_{x4} alone or mCherry_{x4} fused to SV40 NLS was used as negative or positive control, respectively. Transiently expressed free GFP indicates cellular structures, and the boxed areas are enlarged to highlight host nuclei. For each section, a representative of 30 imaging fields is shown. (Scale bars, 20 μ m.)

need to bind to NTRs, which mediate transport across the NPC channel through direct interactions with the NPC components (50). Because our observations indicated that VirE2 does not contain a functional NLS and may not interact with importin α , VirE2 may interact with other NPC components to pass through the nuclear envelope.

The NPC is constructed of multiple copies of ~ 30 different proteins called nucleoporins (Nups). Among them, a group of phenylalanine-glycine-rich nucleoporins (FG-Nups) reside inside the central channel of the NPC and form a continuous interacting surface for NTR-cargo complexes throughout the pore (51). The NTR-cargo complex docks to the NPC by interacting with FG-Nups, which transport the complex through the NPC channel (50).

Ten different FG-Nups have been identified in *A. thaliana* (52). We tested the interactions between VirE2 and each of these FG-Nups using yeast two-hybrid assays. In these assays, the

FG-Nups were expressed as translational fusions to the GAL4 AD. As shown in Fig. 3A and SI Appendix, Fig. S5A, VirE2 specifically interacted with the nucleoporin CG1 in the yeast two-hybrid assays. To confirm the interaction further, we performed pull-down assays using maltose-binding protein (MBP)-tagged CG1 as the bait and VirE2 as the prey. Pull-down and immunoblot assays showed that VirE2 could be precipitated by MBP-tagged CG1, but not by MBP alone, indicating that CG1 interacts directly with VirE2 in vitro (Fig. 3B).

To locate the CG1-interacting domain of VirE2, a series of truncations on VirE2 were generated for the yeast two-hybrid assay. As shown in SI Appendix, Fig. S5B, the N-terminal domain of VirE2 was responsible for its interaction with CG1. In contrast, the C-terminal or putative NLS region of VirE2 alone did not interact with CG1 in the yeast two-hybrid assay, and they did not interfere with the interaction between CG1 and the N-terminal domain of VirE2 significantly (SI Appendix, Fig. S5B).

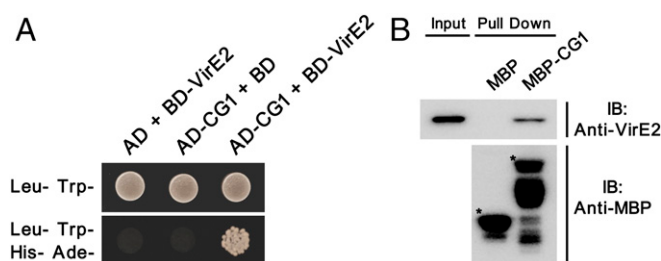


Fig. 3. VirE2 interacts with *A. thaliana* nucleoporin CG1. (A) VirE2 interacted with *A. thaliana* nucleoporin CG1 in a yeast two-hybrid assay. CG1 was expressed as a translational fusion to the GAL4 AD, and VirE2 was expressed as a translational fusion to the GAL4 BD. (B) VirE2 interacts with *A. thaliana* nucleoporin CG1 in MBP pull-down assays. CG1 fused onto MBP or MBP alone was used as the bait and VirE2 was used as the prey in the pull-down assays. The pull-down fractions and 10% of the input were analyzed by Western blot. Free MBP and the MBP-CG1 fusion protein are indicated by asterisks. IB, immunoblot.

In contrast, we did not observe interaction between VirD2 and any of the tested FG-Nups in the yeast two-hybrid assays (*SI Appendix, Fig. S6*). VirD2 is therefore likely imported into the host nucleus using an importin-dependent pathway.

CG1 Is Important for the Nuclear Import of VirE2 and AMT in Plant Cells. Interactions with FG-Nups enable NTRs to translocate through the NPC and bring NTRs into the nucleus (50). Thus, interaction with the nucleoporin CG1 may also assist VirE2 to pass through the NPC channel. To investigate this, we examined whether CG1 is required for nuclear import of VirE2 in *N. benthamiana* leaf epidermal cells. Two genes encoding CG1 homologs are encoded by the *N. benthamiana* genome and are hereafter named *NbCG1A* and *NbCG1B* (*SI Appendix, Fig. S8*). Both of the two protein homologs, *NbCG1A* and *NbCG1B*, show ~38% identity to *A. thaliana* CG1 (*SI Appendix, Fig. S7*).

We first investigated the interactions between VirE2 and the two CG1 homologs from *N. benthamiana*. As shown in Fig. 4A, yeast two-hybrid results showed that VirE2 could interact with both *NbCG1A* and *NbCG1B*, indicating a potentially conserved role of CG1 in the AMT process for these plant species. The interactions were further confirmed by pull-down assays using MBP-tagged *NbCG1A* and *NbCG1B*. As shown in Fig. 4B, VirE2 could be precipitated by MBP-tagged *NbCG1A* and *NbCG1B*, but not by MBP alone, indicating that VirE2 could interact directly with both *NbCG1A* and *NbCG1B* in vitro.

The recombinant tobacco rattle virus (TRV)-based virus-induced gene silencing (VIGS) strategy was then used to silence *NbCG1A* and *NbCG1B* in *N. benthamiana* plants (53). A conserved region of these two genes was chosen to generate a TRV construct to target the expression of the two genes simultaneously (*SI Appendix, Fig. S8*), and transgenic *N. benthamiana* (Nb308A) plants were inoculated with the TRV construct. Three weeks after viral inoculation, the steady-state transcript abundance of these two genes was verified by quantitative RT-PCR (RT-qPCR) using a pair of primers targeting a conserved region of the two genes. As shown in Fig. 4C, expression of both *NbCG1A* and *NbCG1B* was strongly reduced in *NbCG1A/NbCG1B*-silenced plants, compared with the empty vector control. To investigate further the role of CG1 in the nuclear import of VirE2, *A. tumefaciens* XYA105VirE2::GFP11 containing the binary plasmid pXY01 was infiltrated into the *NbCG1A/NbCG1B*-silenced plants. As shown in Fig. 4D and E, nuclear import of VirE2 was impaired in the *NbCG1A/NbCG1B*-silenced plants as compared with the control group, suggesting that CG1 is important for the nuclear uptake of *Agrobacterium*-delivered VirE2 in *N. benthamiana* plants.

To determine whether CG1 is required for the AMT process, a transient transformation assay, based on transient expression of GFP from the T-DNA, was conducted on the leaves of the *NbCG1A/NbCG1B*-silenced *N. benthamiana* plants. As shown in Fig. 4F and G, the intensity of transiently expressed GFP from T-DNA decreased in the *NbCG1A/NbCG1B*-silenced plants compared with the control, indicating that silencing of *NbCG1A* and *NbCG1B* in *N. benthamiana* plants reduced the efficiency of transient transformation mediated by *Agrobacterium*. These results indicate that CG1 is important for *Agrobacterium*-mediated transient transformation of *N. benthamiana* leaf cells.

To confirm further the importance of host CG1 in the AMT process, an *Arabidopsis* mutant line was obtained with a T-DNA insertion in the fourth intron of *CG1* (*SI Appendix, Fig. S9A and B*). The absence of *CG1* transcripts in this mutant line was confirmed by RT-PCR (*SI Appendix, Fig. S9C*), and no obvious growth defect of this mutant line was observed compared to that of the wild-type (Col-0) control. A root transformation assay was then carried out to examine the AMT efficiency. As shown in Fig. 5A and B, the *cgl-1* mutant displayed significantly attenuated tumor formation efficiency as compared to the wild-type control, indicating that the host CG1 is involved in the AMT process. Taken together, our results demonstrate that VirE2 interacts with the host nucleoporin CG1 to facilitate its nuclear uptake and the transformation process.

Discussion

Agrobacterium has long been used as an important tool to deliver DNA into various cells. Under natural conditions, this bacterium can transfer a 10- to 20-kb T-DNA into the host nucleus. Transfer of an even longer artificial T-DNA fragment of 150 kb has also been reported (54). As estimated, VirE2 can coat ssDNA in vitro to form a filamentous VirE2-ssDNA complex with an outer diameter of 12.6 nm, which has a 4.4-nm helical pitch; each turn of the filament coil contains 3.4 VirE2 molecules and 63.6 DNA bases (55). Based on this calculation, the theoretical length of the T-complex can reach 1.7 μ m for the nopaline *Agrobacterium* strain C58 (with ~24-kb T-DNA) or 10 μ m for the 150-kb artificial T-DNA. The NPC has an exclusion size limit of 23 to 39 nm during the active nuclear uptake process (56). Thus, it is likely that the T-complex adopts a polar translocation mode to pass through the NPC channel. However, it is not clear how this polar transport is coordinated and what roles VirD2 and VirE2 play in this process.

Here, we provide data suggesting a VirD2-piloting and VirE2-assisting model for the nuclear import of the T-complex in host cells (Fig. 6). We propose that upon assembly in the host cytoplasm, the T-complex is piloted to the nuclear pore by VirD2 through interactions with host importins. Interactions of importin β with the FG-Nups initiate the translocation and bring the “head” of the T-complex into the NPC channel, which enables the docking of T-DNA-associated VirE2 to the nucleoporin CG1. Interactions of VirE2 with CG1 may provide lateral assistance to facilitate the T-complex to enter and pass through the channel.

Nucleoporins can be hijacked by a variety of viruses for trafficking of viral proteins and genomes into and out of the host nucleus (57). Our results here represent an example of bacterial derived virulence factors that combine importin- and nucleoporin-dependent mechanisms to deliver a nucleoprotein complex into the nucleus. Our findings suggest a molecular machinery for nuclear import of large cargos and may further provide approaches for targeted nuclear import of large protein or nucleoprotein complexes in eukaryotic cells.

CG1 is located at the cytoplasmic side of the NPC (52). Thus, interactions between VirE2 and CG1 may occur at the entrance of the NPC and promote entry of the T-complex into the NPC channel. Our results show that *Agrobacterium*-delivered VirE2

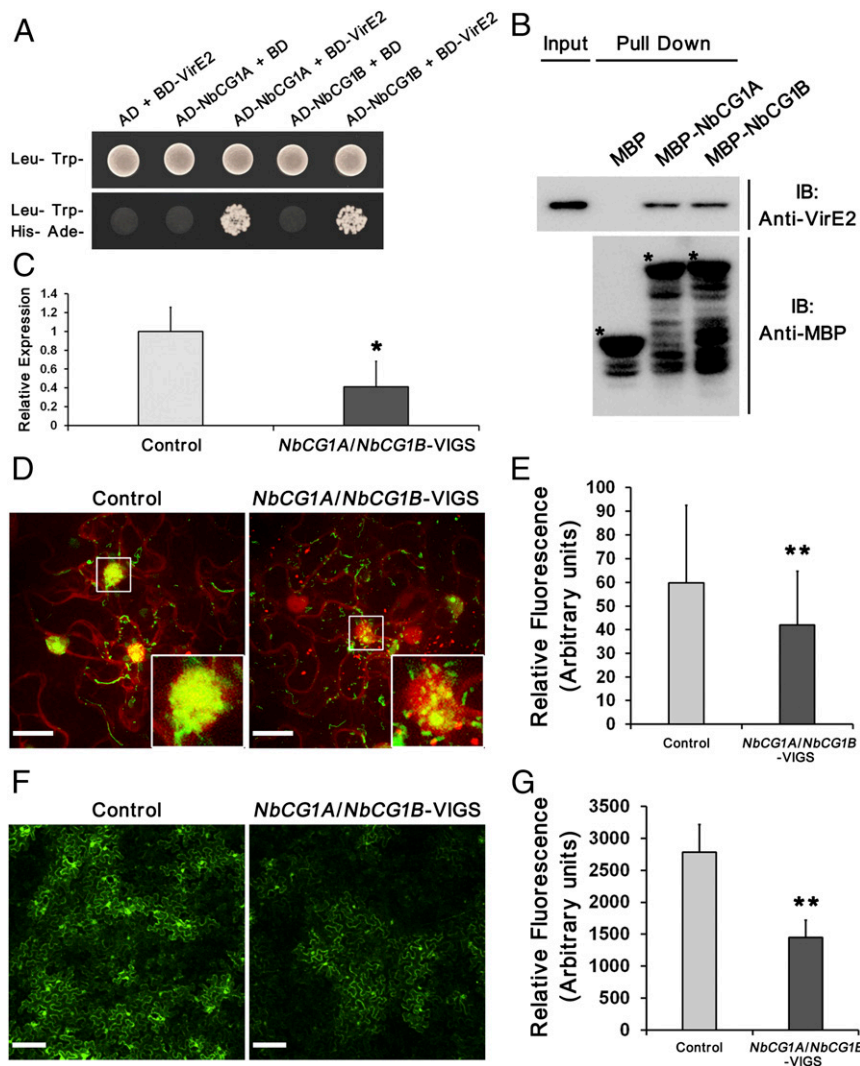


Fig. 4. CG1 is important for the nuclear import of VirE2 and *Agrobacterium*-mediated transient transformation of *N. benthamiana* leaf cells. (A) VirE2 interacts with the *N. benthamiana* CG1 homologs NbCG1A and NbCG1B in yeast two-hybrid assays. NbCG1A and NbCG1B were expressed as translational fusions to the GAL4 AD, and VirE2 was expressed as a translational fusion to the GAL4 BD. (B) VirE2 interacts with NbCG1A and NbCG1B in MBP pull-down assays. NbCG1A and NbCG1B fused to MBP were used as the baits, and VirE2 was used as the prey in the pull-down assays. The pull-down fractions and 10% of the input were analyzed by Western blot. Free MBP and MBP-fused baits are marked by an asterisk. IB, immunoblot. (C) VIGS of NbCG1A and NbCG1B in transgenic *N. benthamiana* (Nb308A) plants. The relative steady-state level of NbCG1A and NbCG1B transcripts was determined by RT-qPCR for each sample at 3 wk after virus inoculation. Samples were normalized to endogenous NbActin. The empty vector was used as the control. Data are presented as means \pm SDs of $n = 5$ independent plants. $*P < 0.05$. (D) CG1 is important for the nuclear import of VirE2 in *N. benthamiana* leaf cells. Three weeks after virus inoculation, mature leaves were agroinfiltrated with *A. tumefaciens* XYA105:VirE2::GFP11 containing the binary plasmid pXY01. The boxed areas are enlarged to highlight host nuclei. (Scale bars, 20 μ m.) (E) The fluorescence intensity of VirE2-GFP_{comp} signals was measured in each host nucleus. Data are presented as the means \pm SD of $n = 60$ independent samples. $**P < 0.01$. (F) CG1 is important for *Agrobacterium*-mediated transient transformation of *N. benthamiana* leaf cells. Three weeks after virus inoculation, mature leaves were agroinfiltrated with *A. tumefaciens* XYA105 containing the binary plasmid pXY01-GFP (expressing free GFP under the control of a CaMV 35S promoter). (Scale bars, 100 μ m.) (G) The fluorescence intensity of transiently expressed GFP was measured in each image. Data are presented as means \pm SDs of $n = 30$ independent samples. $**P < 0.01$.

could not enter the host nucleus in the absence of VirD2 or T-DNA (Fig. 1), indicating that the VirE2-interacting site(s) on CG1 may reside inside the NPC channel and may not be exposed to the cytoplasmic side. Thus, only VirD2 can initiate T-complex translocation into the NPC channel. Because VirE2 is the most abundant virulence effector protein that accumulates in induced *Agrobacterium* cells (58), it is likely that VirE2 would be delivered into host cells in an excessive amount. Thus, interactions occurring between CG1 and T-DNA-bound VirE2 rather than free VirE2 would avoid the competition between unbound VirE2 and the VirE2-coated T-complex in nuclear import and maximize the utility efficiency of host resources for the bacteria.

Although VirE2 expressed *in planta* cannot localize to the nucleus (SI Appendix, Fig. S2A and C), *in planta* expression of VirE2 can complement the transformation deficiency of an *Agrobacterium virE2* mutant strain (34). Apparently, in the presence of both VirD2 and T-strands, VirE2 localized in the plant cytoplasm can enter the nucleus (SI Appendix, Fig. S2B and C). This result indicates that plant-expressed VirE2 is targeted into the nucleus in the same way as is *Agrobacterium*-delivered VirE2.

VirD2 was reported to interact with several *Arabidopsis* importin α isoforms including IMPA-1, IMPA-2, IMPA-3, and IMPA-4 (30, 31). Our results here show that VirD2 could interact with additional two importin α isoforms including IMPA-6 and

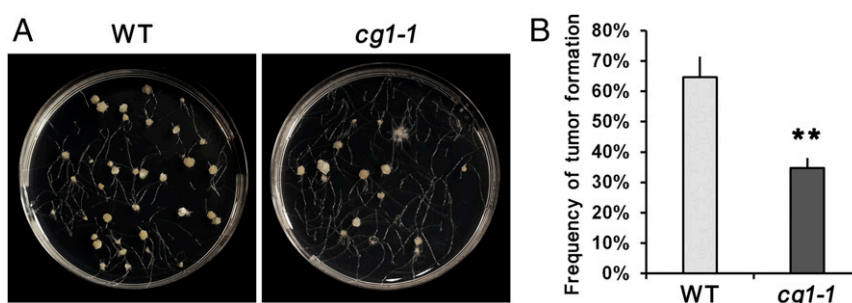


Fig. 5. CG1 is important for *Agrobacterium*-mediated stable transformation of *A. thaliana* root segments. (A) The *cg1-1* mutation attenuated tumorigenesis in the root transformation assay. (B) Quantification of the frequency of tumor formation. Data are presented as means \pm SDs based on the number of tumors formed on 150 root segments. ** $P < 0.01$.

IMPA-7. We found that the two putative NLSs of VirE2 could not function inside plant cells, which is consistent with a recent study showing that the NLSs of VirE2 only had weak affinity to plant importin α and were not likely to be functional *in vivo* (35). Thus, the previously observed *in planta* interactions between VirE2 and *Arabidopsis* importin α isoforms (31, 59) might have been a result of the overexpression of these proteins. Deletions of the NLSs of VirE2 were shown to affect the nuclear import of a GUS-VirE2 reporter (34); however, this might also have resulted from structural changes caused by these mutations and requires further studies. Nevertheless, our data indicate that VirD2–importin α and VirE2–CG1 interactions are the two major forces responsible for VirE2 nuclear import.

Both VirD2 and VirE2 are required for efficient nuclear import of T-DNA in host cells. VirD2 and VirE2 may perform complementary functions and exploit different host factors for their nuclear import (41). Considering that VirD2 is outnumbered by VirE2 in the T-complex, interactions with the same host proteins might cause competition between these two effectors and jeopardize the pilot role of VirD2 in polar transport of the T-complex into the host nucleus. We hypothesize that the T-complex is targeted into the nucleus by a “head” guide from the VirD2–importin interaction and a lateral assistance from the VirE2–nucleoporin interaction in a noncompeting fashion.

The *cg1-1* mutant displayed attenuated tumor formation efficiency, indicating that interaction between VirE2 and CG1 might play an assisting rather than essential role only in the nuclear import process of the T-complex. In contrast, deletion of *virE2* causes a more significant effect on the transformation of plant cells (42), presumably due to the disruption of VirE2 functions involved in multiple steps of the transformation process such as nuclear import, T-DNA protection, and cytoplasmic trafficking. Consequently, elimination of CG1 has a much less significant effect on transformation than does elimination of VirE2. VirE2 can be substituted by GALLS protein from some *Agrobacterium rhizogenes* strains (60). It would be interesting to determine the possible role of FG-Nups in nuclear import of GALLS protein.

Our results suggest that transport of VirE2 through the NPC channel is assisted by direct interactions between VirE2 and the FG-Nup CG1, which may mimic the transport mode of host NTRs. Many NTRs, including importin β , are composed of a tandem series of HEAT repeats, which form solenoid structures (61). The HEAT repeat composition is hypothesized to provide different levels of structural elasticity, which enables the NTRs to adopt helicoidal structures and facilitates their transport through the NPC channel. Interestingly, VirE2 can self-interact in a “head-to-tail” manner and also forms repeated solenoid structures (55, 62). Thus, the structural similarity between the

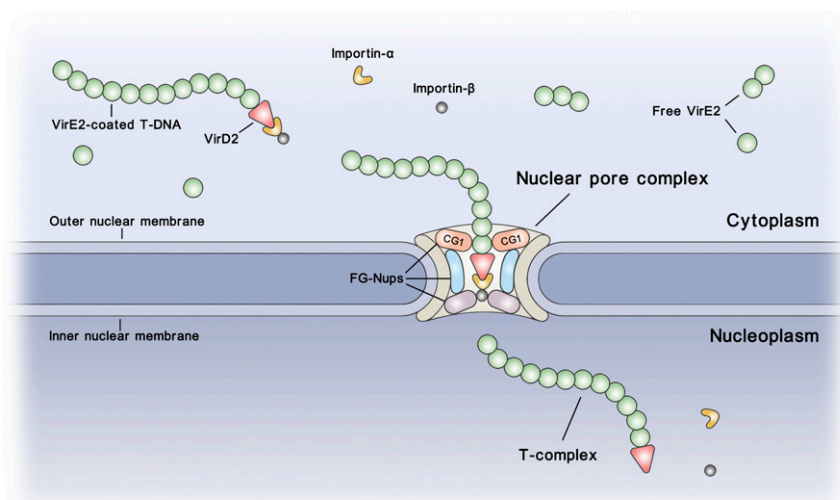


Fig. 6. A hypothetical model for the nuclear import of the T-complex. VirE2 coats the VirD2-associated T-DNA to form the T-complex inside the host cytoplasm. After that, VirD2 interacts with host importins to guide the “head” of this nucleoprotein complex to the host nuclear pore. Interactions of importin β with the NPC components initiate the translocation of the T-complex into the channel, which further enables the interactions between T-DNA-associated VirE2 and the nucleoporin CG1. Finally, interactions of VirE2 with CG1 facilitate the T-complex on the lateral side of the T-complex to enter and pass through the NPC channel. Inside the host nucleus, the T-complex is separated from the importins and can further target the host chromosomes for integration.

VirE2-coated T-complex and the NTRs indicates that VirE2 may mimic NTRs and facilitate the transport of the T-DNA through the NPC channel by coating it and shaping it in a transferable form, as proposed previously (41).

Materials and Methods

For details on *A. tumefaciens* mutant construction and plasmid construction, please refer to [SI Appendix](#).

Strains, Plasmids, Primers, and Growth Conditions. *A. tumefaciens* strains, plasmids, and primers used in this study are listed in [SI Appendix, Tables S1–S3](#), respectively. *A. tumefaciens* strains were grown at 28 °C in Luria-Bertani (LB) medium supplemented with kanamycin (50 µg·mL⁻¹) as necessary. The yeast strain AH109 was cultured in YPGA medium.

Plant Materials and Growth Conditions. *A. thaliana* wild-type (Col-0) and mutant plants were used in the root transformation assay. The *CG1* insertional mutants *cg1-1* (CS803687) was obtained from the *Arabidopsis* Biological Resource Center at Ohio State University. *N. benthamiana* wild-type, transgenic line Nb308A (expressing GFP1–10 and DsRed), transgenic line Nb308E2 (expressing VirE2-GFP11, GFP1–10, and DsRed) plants were used for agroinfiltration. All of the plants were grown at 22 °C under a 16-h light/8-h dark photoperiod.

Agroinfiltration. *N. benthamiana* plants were used for agroinfiltration experiments. *A. tumefaciens* strains grown overnight were harvested and diluted in fresh LB medium to a final concentration of ~10⁸ cfu/mL (OD₆₀₀ = 0.1) and grown for an additional 6 to 8 h. The bacteria were harvested, resuspended in H₂O, and infiltrated into the underside of fully expanded *N. benthamiana* leaves using a syringe. For detection of *Agrobacterium*-delivered VirE2, transient expression of mCherry_{x4}-labeled peptides or the transient transformation assay of GFP, *A. tumefaciens* strains were infiltrated into *N. benthamiana* leaves at a final concentration of ~10⁹, 5 × 10⁸, or 5 × 10⁷ cfu/mL (OD₆₀₀ = 1.0, 0.5, or 0.05), respectively. Agroinfiltration experiments to express VirE2-Venus *in planta* were conducted using *A. tumefaciens* At2065 as previously described (38).

Yeast Two-Hybrid Assay. Yeast two-hybrid assays were performed following the user manual (Clontech). Briefly, constructed plasmids were introduced into yeast strain AH109 through a lithium acetate-mediated transformation and the transformants were selected on SD/-Leu/-Trp medium with agar. The transformed yeast cells were then cultured overnight in SD/-Leu/-Trp liquid medium. The cultured yeast cells were washed twice and resuspended with H₂O, which were subsequently spotted onto the SD/-Leu/-Trp, SD/-His/-Leu/-Trp, or SD/-Ade/-His/-Leu/-Trp plates with a final concentration of ~3 × 10⁷ cfu/mL (OD₆₀₀ = 1). The plates were incubated at 30 °C.

Pull-Down Assay. *Escherichia coli* BL21(DE3) was used for protein expression. Briefly, *E. coli* strains containing the corresponding plasmids were grown to midlog phase (OD₆₀₀ = 0.6), isopropyl-β-D-thiogalactoside (IPTG) was then added into the cell cultures to a final concentration of 1 mM, and the cells were grown at 28 °C for 5 h. Bacterial cells were resuspended in lysis buffer (50 mM Tris-HCl, 100 mM NaCl, pH 7.5) containing protease inhibitors (supplied by Nacalai Tesque) and lysed by sonication. Cell debris was removed by centrifugation at 15,000 × *g* for 15 min at 4 °C. The supernatant solution containing bait proteins was incubated with 80 µL of amylose resin from New England Biolabs (MBP-based pull-down assay) or 80 µL of glutathione agarose resin from GoldBio (GST-based pull-down assay) at 4 °C for 4 h. The column was washed five times with lysis buffer. After that, the supernatant solution of the prey proteins (VirE2 or VirD2) was added to the column and incubated on a rotator at 4 °C overnight. The column was washed five times with the lysis buffer and captured proteins were eluted with lysis buffer containing 10 mM maltose (MBP-based pull-down assay) or 10 mM reduced glutathione (GST-based pull-down assay). The eluted

proteins were analyzed by 10% SDS/PAGE under reducing conditions followed by InstantBlue (Expedeon) staining or Western blot analysis with the appropriate antibodies as indicated.

FIGS. *A. tumefaciens* GV3101(pMP90) containing the binary plasmid pTRV1, pTRV2, and pTRV2-NbCG1A/NbCG1B were grown overnight in LB medium. The cells were harvested and diluted in fresh LB medium to a final concentration of ~10⁸ cfu/mL (OD₆₀₀ = 0.1) and grown for an additional 6 to 8 h. *A. tumefaciens* strains harboring pTRV2 or pTRV2-NbCG1A/NbCG1B were mixed at a ratio of 1:1 with an *A. tumefaciens* strain containing pTRV1 to a final concentration of ~5 × 10⁸ cfu/mL (OD₆₀₀ = 0.5) in H₂O. The bacteria were infiltrated into the lower leaves of six-leaf-stage *N. benthamiana* plants (Nb308A) using a syringe.

RT-qPCR Analysis. Three weeks post viral inoculation, total RNA was isolated from *N. benthamiana* leaves using a TRIzol-based method followed by first-strand cDNA synthesis using a RevertAid First Strand cDNA Synthesis Kit (Thermo Scientific). RT-qPCR was performed with KAPA SYBR FAST qPCR Master Mix (2×) Kit (Kapa Biosystems). Expression of *NbCG1A/NbCG1B* was examined using the primer pair RT1001/RT1002. Expression of endogenous *NbActin* (NCBI accession number AY179605) was examined using the primer pair RT1003/RT1004.

Root Transformation Assay. *A. thaliana* wild-type (Col-0) or mutant seeds were surface-sterilized using 15% bleach solution and incubated at 4 °C for 2 d. The seeds were placed onto solidified 1/2× Murashige and Skoog (MS) medium (supplemented with 1% sucrose and MES [0.5 g·L⁻¹], pH 5.8) and incubated under a 16-h light/8-h dark photoperiod at 22 °C for 10 d. Roots from individual seedlings were cut into segments and mixed with 1 mL of *A. tumefaciens* cells (A348) at a concentration of 10⁸ cfu/mL (OD₆₀₀ = 0.1) and spread onto a solidified 1/2× MS plate. The plates were subsequently incubated at 22 °C for 24 h. The root segments were then aligned onto 1/2× MS medium plates containing cefotaxime (100 µg·mL⁻¹) and kept at 22 °C for 5 wk.

Bimolecular Fluorescence Complementation. Tobacco BY-2 protoplasts were generated and electroporated with 10 µg of DNA from each plasmid as previously described (59). The bimolecular fluorescence complementation vector constructs were described previously (59, 63).

Confocal Microscopy and Quantification of Fluorescence Intensity. A PerkinElmer UltraView Vox Spinning Disk system with electron-multiplying charge-coupled device cameras was used for confocal microscopy. All images were captured at 2 d postagroinfiltration and processed by Volocity 3D Image Analysis Software 6.2.1. Images for the transient transformation assay of GFP were obtained 2 d after agroinfiltration under confocal microscopy with an Olympus UPL SAPO 10× numerical aperture (N.A.) 0.40 objective. Detection of *Agrobacterium*-delivered VirE2 and transient expression of mCherry_{x4}-labeled peptides were performed using an Olympus UPLSAPO 60× N.A. 1.20 water-immersion objective. Fluorescence intensity was measured using ImageJ (<https://imagej.nih.gov/ij/>).

Statistical Analysis. Quantitative data are presented as means ± SD. When appropriate, statistical differences between groups were analyzed using an unpaired Student's *t* test.

Data Availability. All study data are included in the article and [SI Appendix](#).

ACKNOWLEDGMENTS. We thank Michelle Mok Lim Sum and Yan Tong for technical assistance. This work was supported in part by grants from the Singapore Ministry of Education (R-154-000-B22-114, R-154-000-B68-114, and R-154-000-C10-114) and the National Natural Science Foundation of China (Grants 31700118 and 31870117). Work in the S.B.G. laboratory was supported by grants from the National Science Foundation.

1. L. M. Albright, M. F. Yanofsky, B. Leroux, D. Q. Ma, E. W. Nester, Processing of the T-DNA of *Agrobacterium tumefaciens* generates border nicks and linear, single-stranded T-DNA. *J. Bacteriol.* **169**, 1046–1055 (1987).
2. P. Zambryski *et al.*, Tumor DNA structure in plant cells transformed by *A. tumefaciens*. *Science* **209**, 1385–1391 (1980).
3. M. D. Chilton *et al.*, Stable incorporation of plasmid DNA into higher plant cells: The molecular basis of crown gall tumorigenesis. *Cell* **11**, 263–271 (1977).
4. P. Bundock, A. den Dulk-Ras, A. Beijersbergen, P. J. Hooykaas, Trans-kingdom T-DNA transfer from *Agrobacterium tumefaciens* to *Saccharomyces cerevisiae*. *EMBO J.* **14**, 3206–3214 (1995).

5. K. L. Piers, J. D. Heath, X. Liang, K. M. Stephens, E. W. Nester, *Agrobacterium tumefaciens*-mediated transformation of yeast. *Proc. Natl. Acad. Sci. U.S.A.* **93**, 1613–1618 (1996).
6. M. J. de Groot, P. Bundock, P. J. Hooykaas, A. G. Beijersbergen, *Agrobacterium tumefaciens*-mediated transformation of filamentous fungi. *Nat. Biotechnol.* **16**, 839–842 (1998).
7. S. Kathiresan, A. Chandrashekar, G. A. Ravishanker, R. Sarada, *Agrobacterium*-mediated transformation in the green alga *Haematococcus pluvialis* (chlorophyceae, volvocales). *J. Phycol.* **45**, 642–649 (2009).

8. C. B. Michielse, P. J. Hooykaas, C. A. van den Hondel, A. F. Ram, *Agrobacterium*-mediated transformation as a tool for functional genomics in fungi. *Curr. Genet.* **48**, 1–17 (2005).
9. T. Tzfira, V. Citovsky, *Agrobacterium*-mediated genetic transformation of plants: Biology and biotechnology. *Curr. Opin. Biotechnol.* **17**, 147–154 (2006).
10. K. Wang, L. Herrera-Estrella, M. Van Montagu, P. Zambryski, Right 25 bp terminus sequence of the nopaline T-DNA is essential for and determines direction of DNA transfer from *Agrobacterium* to the plant genome. *Cell* **38**, 455–462 (1984).
11. P. Scheffele, W. Pansegrau, E. Lanka, Initiation of *Agrobacterium tumefaciens* T-DNA processing. Purified proteins VirD1 and VirD2 catalyze site- and strand-specific cleavage of superhelical T-border DNA *in vitro*. *J. Biol. Chem.* **270**, 1269–1276 (1995).
12. M. F. Yanofsky *et al.*, The *virD* operon of *Agrobacterium tumefaciens* encodes a site-specific endonuclease. *Cell* **47**, 471–477 (1986).
13. E. Cascales, P. J. Christie, The versatile bacterial type IV secretion systems. *Nat. Rev. Microbiol.* **1**, 137–149 (2003).
14. E. Cascales, P. J. Christie, Definition of a bacterial type IV secretion pathway for a DNA substrate. *Science* **304**, 1170–1173 (2004).
15. P. J. Christie, J. E. Ward, S. C. Winans, E. W. Nester, The *Agrobacterium tumefaciens* *virE2* gene product is a single-stranded-DNA-binding protein that associates with T-DNA. *J. Bacteriol.* **170**, 2659–2667 (1988).
16. V. Citovsky, M. L. Wong, P. Zambryski, Cooperative interaction of *Agrobacterium* VirE2 protein with single-stranded DNA: Implications for the T-DNA transfer process. *Proc. Natl. Acad. Sci. U.S.A.* **86**, 1193–1197 (1989).
17. P. Sen, G. J. Pazour, D. Anderson, A. Das, Cooperative binding of *Agrobacterium tumefaciens* VirE2 protein to single-stranded DNA. *J. Bacteriol.* **171**, 2573–2580 (1989).
18. L. Rossi, B. Hohn, B. Tinland, Integration of complete transferred DNA units is dependent on the activity of virulence E2 protein of *Agrobacterium tumefaciens*. *Proc. Natl. Acad. Sci. U.S.A.* **93**, 126–130 (1996).
19. V. M. Yusibov, T. R. Steck, V. Gupta, S. B. Gelvin, Association of single-stranded transferred DNA from *Agrobacterium tumefaciens* with tobacco cells. *Proc. Natl. Acad. Sci. U.S.A.* **91**, 2994–2998 (1994).
20. X. Li, S. Q. Pan, *Agrobacterium* delivers VirE2 protein into host cells via clathrin-mediated endocytosis. *Sci. Adv.* **3**, e1601528 (2017).
21. Q. Yang, X. Li, H. Tu, S. Q. Pan, *Agrobacterium*-delivered virulence protein VirE2 is trafficked inside host cells via a myosin XI-K-powered ER/actin network. *Proc. Natl. Acad. Sci. U.S.A.* **114**, 2982–2987 (2017).
22. X. Li, H. Tu, S. Q. Pan, *Agrobacterium* delivers anchorage protein VirE3 for companion VirE2 to aggregate at host entry sites for T-DNA protection. *Cell Rep.* **25**, 302–311.e6 (2018).
23. T. Tzfira, B. Lacroix, V. Citovsky, “Nuclear import of *agrobacterium* T-DNA” in *Nuclear Import and Export in Plants and Animals*, T. Tzfira, V. Citovsky, Eds. (Springer, Boston, MA, 2005), pp. 83–99.
24. L. F. Pemberton, B. M. Paschal, Mechanisms of receptor-mediated nuclear import and nuclear export. *Traffic* **6**, 187–198 (2005).
25. N. Freitas, C. Cunha, Mechanisms and signals for the nuclear import of proteins. *Curr. Genomics* **10**, 550–557 (2009).
26. B. Tinland, Z. Koukoliková-Nicola, M. N. Hall, B. Hohn, The T-DNA-linked VirD2 protein contains two distinct functional nuclear localization signals. *Proc. Natl. Acad. Sci. U.S.A.* **89**, 7442–7446 (1992).
27. C. E. Shurvinton, L. Hodges, W. Ream, A nuclear localization signal and the C-terminal omega sequence in the *Agrobacterium tumefaciens* VirD2 endonuclease are important for tumor formation. *Proc. Natl. Acad. Sci. U.S.A.* **89**, 11837–11841 (1992).
28. E. A. Howard, J. R. Zupan, V. Citovsky, P. C. Zambryski, The VirD2 protein of *A. tumefaciens* contains a C-terminal bipartite nuclear localization signal: Implications for nuclear uptake of DNA in plant cells. *Cell* **68**, 109–118 (1992).
29. L. Rossi, B. Hohn, B. Tinland, The VirD2 protein of *Agrobacterium tumefaciens* carries nuclear localization signals important for transfer of T-DNA to plant. *Mol. Gen. Genet.* **239**, 345–353 (1993).
30. N. Ballas, V. Citovsky, Nuclear localization signal binding protein from *Arabidopsis* mediates nuclear import of *Agrobacterium* VirD2 protein. *Proc. Natl. Acad. Sci. U.S.A.* **94**, 10723–10728 (1997).
31. S. Bhattacharjee *et al.*, IMPa-4, an *Arabidopsis* importin alpha isoform, is preferentially involved in *Agrobacterium*-mediated plant transformation. *Plant Cell* **20**, 2661–2680 (2008).
32. T. Tzfira, V. Citovsky, Comparison between nuclear localization of nopaline- and octopine-specific *Agrobacterium* VirE2 proteins in plant, yeast and mammalian cells. *Mol. Plant Pathol.* **2**, 171–176 (2001).
33. S. B. Gelvin, Finding a way to the nucleus. *Curr. Opin. Microbiol.* **13**, 53–58 (2010).
34. V. Citovsky, J. Zupan, D. Warnick, P. Zambryski, Nuclear localization of *Agrobacterium* VirE2 protein in plant cells. *Science* **256**, 1802–1805 (1992).
35. C. W. Chang, S. J. Williams, R. M. Couñago, B. Kobe, Structural basis of interaction of bipartite nuclear localization signal from *Agrobacterium* VirD2 with rice importin- α . *Mol. Plant* **7**, 1061–1064 (2014).
36. T. Tzfira, M. Vaidya, V. Citovsky, VIP1, an *Arabidopsis* protein that interacts with *Agrobacterium* VirE2, is involved in VirE2 nuclear import and *Agrobacterium* infectivity. *EMBO J.* **20**, 3596–3607 (2001).
37. B. Lacroix, M. Vaidya, T. Tzfira, V. Citovsky, The VirE3 protein of *Agrobacterium* mimics a host cell function required for plant genetic transformation. *EMBO J.* **24**, 428–437 (2005).
38. Y. Shi, L. Y. Lee, S. B. Gelvin, Is VIP1 important for *Agrobacterium*-mediated transformation? *Plant J.* **79**, 848–860 (2014).
39. R. Lapham *et al.*, VIP1 and its homologs are not required for *Agrobacterium*-mediated transformation, but play a role in *Botrytis* and salt stress responses. *Front. Plant Sci.* **9**, 749 (2018).
40. X. Li, T. Zhu, H. Tu, S. Q. Pan, *Agrobacterium* VirE3 Uses its two tandem domains at the C-terminus to retain its companion VirE2 on the cytoplasmic side of the host plasma membrane. *Front. Plant Sci.* **11**, 464 (2020).
41. A. Ziemienowicz, T. Merkle, F. Schoumacher, B. Hohn, L. Rossi, Import of *Agrobacterium* T-DNA into plant nuclei: Two distinct functions of VirD2 and VirE2 proteins. *Plant Cell* **13**, 369–383 (2001).
42. X. Li, Q. Yang, H. Tu, Z. Lim, S. Q. Pan, Direct visualization of *Agrobacterium*-delivered VirE2 in recipient cells. *Plant J.* **77**, 487–495 (2014).
43. H. Tu, X. Li, Q. Yang, L. Peng, S. Q. Pan, Real-time trafficking of *Agrobacterium* virulence protein VirE2 inside host cells. *Curr. Top. Microbiol. Immunol.* **418**, 261–286 (2018).
44. E. E. Hood, S. B. Gelvin, L. S. Melchers, A. Hoekema, New *Agrobacterium* helper plasmids for gene transfer to plants. *Transgenic Res.* **2**, 208–218 (1993).
45. R. B. Horsch, H. J. Klee, Rapid assay of foreign gene expression in leaf discs transformed by *Agrobacterium tumefaciens*: Role of T-DNA borders in the transfer process. *Proc. Natl. Acad. Sci. U.S.A.* **83**, 4428–4432 (1986).
46. K. E. Knockenhauer, T. U. Schwartz, The nuclear pore complex as a flexible and dynamic gate. *Cell* **164**, 1162–1171 (2016).
47. S. R. Wente, M. P. Rout, The nuclear pore complex and nuclear transport. *Cold Spring Harb. Perspect. Biol.* **2**, a000562 (2010).
48. B. L. Timney *et al.*, Simple rules for passive diffusion through the nuclear pore complex. *J. Cell Biol.* **215**, 57–76 (2016).
49. N. Mosammaparast, L. F. Pemberton, Karyopherins: From nuclear-transport mediators to nuclear-function regulators. *Trends Cell Biol.* **14**, 547–556 (2004).
50. I. V. Aramburu, E. A. Lemke, Floppy but not sloppy: Interaction mechanism of FG-nucleoporins and nuclear transport receptors. *Semin. Cell Dev. Biol.* **68**, 34–41 (2017).
51. L. J. Terry, S. R. Wente, Flexible gates: Dynamic topologies and functions for FG nucleoporins in nucleocytoplasmic transport. *Eukaryot. Cell* **8**, 1814–1827 (2009).
52. K. Tamura, Y. Fukao, M. Iwamoto, T. Haraguchi, I. Hara-Nishimura, Identification and characterization of nuclear pore complex components in *Arabidopsis thaliana*. *Plant Cell* **22**, 4084–4097 (2010).
53. Y. Liu, M. Schiff, R. Marathe, S. P. Dinesh-Kumar, Tobacco *Rar1*, *EDS1* and *NPR1/NIM1* like genes are required for N-mediated resistance to tobacco mosaic virus. *Plant J.* **30**, 415–429 (2002).
54. A. Frary, C. M. Hamilton, Efficiency and stability of high molecular weight DNA transformation: An analysis in tomato. *Transgenic Res.* **10**, 121–132 (2001).
55. V. Citovsky, B. Guralnick, M. N. Simon, J. S. Wall, The molecular structure of *Agrobacterium* VirE2-single stranded DNA complexes involved in nuclear import. *J. Mol. Biol.* **271**, 718–727 (1997).
56. N. Panté, M. Kann, Nuclear pore complex is able to transport macromolecules with diameters of about 39 nm. *Mol. Biol. Cell* **13**, 425–434 (2002).
57. V. Le Sage, A. J. Moulard, Viral subversion of the nuclear pore complex. *Viruses* **5**, 2019–2042 (2013).
58. P. Engström, P. Zambryski, M. Van Montagu, S. Stachel, Characterization of *Agrobacterium tumefaciens* virulence proteins induced by the plant factor acetosyringone. *J. Mol. Biol.* **197**, 635–645 (1987).
59. L. Y. Lee, M. J. Fang, L. Y. Kuang, S. B. Gelvin, Vectors for multi-color bimolecular fluorescence complementation to investigate protein-protein interactions in living plant cells. *Plant Methods* **4**, 24 (2008).
60. L. D. Hodges, J. Cuperus, W. Ream, *Agrobacterium rhizogenes* GALLS protein substitutes for *Agrobacterium tumefaciens* single-stranded DNA-binding protein VirE2. *J. Bacteriol.* **186**, 3065–3077 (2004).
61. S. H. Yoshimura, T. Hirano, HEAT repeats—versatile arrays of amphiphilic helices working in crowded environments? *J. Cell Sci.* **129**, 3963–3970 (2016).
62. O. Dym *et al.*, Crystal structure of the *Agrobacterium* virulence complex VirE1–VirE2 reveals a flexible protein that can accommodate different partners. *Proc. Natl. Acad. Sci. U.S.A.* **105**, 11170–11175 (2008).
63. L. Y. Lee, S. B. Gelvin, Bimolecular fluorescence complementation for imaging protein interactions in plant hosts of microbial pathogens. *Methods Mol. Biol.* **1197**, 185–208 (2014).



Supplementary Information for

***Agrobacterium*-delivered VirE2 interacts with host nucleoporin CG1 to facilitate the nuclear import of VirE2-coated T-complex**

Xiaoyang Li, Qinghua Yang, Ling Peng, Haitao Tu, Lan-Ying Lee, Stanton B. Gelvin and Shen Q. Pan *

* Corresponding Author:
Shen Q. Pan
Email: dbspansq@nus.edu.sg

This PDF file includes:

Supplementary text
Figures S1 to S9
Tables S1 to S3
SI References

Supplementary text

Materials and Methods

A. tumefaciens mutant construction

A. tumefaciens mutants were generated using a *sacB*-based gene replacement strategy (1).

Deletion of individual effector in *A. tumefaciens* strain EHA105virE2::*GFP11*

pEx18Km-ΔVirD2, pEx18Km-ΔVirD5 and pEx18Km-ΔVirF were used to generate *A. tumefaciens* strains EHA105virE2::*GFP11*ΔvirD2, EHA105virE2::*GFP11*ΔvirD5 and EHA105virE2::*GFP11*ΔvirF, respectively, in the background of *A. tumefaciens* strain EHA105virE2::*GFP11*. pEx18Km-ΔVirD5, pEx18Km-ΔVirE2, pEx18Km-ΔVirE3 and pEx18Km-ΔVirF were used to generate *A. tumefaciens* strains XYA105ΔvirD5ΔvirE2ΔvirE3ΔvirF in the background of *A. tumefaciens* strain XYA105. pEx18Km-ΔVirD2, pEx18Km-ΔVirD5, pEx18Km-ΔVirE2, pEx18Km-ΔVirE3 and pEx18Km-ΔVirF were used to generate *A. tumefaciens* strains XYA105ΔvirD2ΔvirD5ΔvirE2ΔvirE3ΔvirF, in the background of *A. tumefaciens* strain XYA105.

XYA105 and XYA105virE2::*GFP11*

The flanking sequences of the T-DNA left border were amplified from the total DNA of *A. tumefaciens* strain EHA105 with primer pair E1001/E1002 or E1003/E1004. The PCR products were further amplified with primer pair E1005/E1006 using overlapping PCR, digested with *Xba*I and *Xho*I, and inserted into pEx18Km to generate pEx18Km-ΔLB. pEx18Km-ΔLB was used to generate *A. tumefaciens* strain XYA105 or XYA105virE2::*GFP11* from the *A. tumefaciens* strain EHA105 or EHA105virE2::*GFP11*, respectively.

Plasmid constructions

Transient expression plasmids

To generate the binary plasmid pXY01-GFP expressing free GFP on T-DNA, the GFP coding sequence was amplified with primer pair P1001/P1002, digested with *Xho*I and *Bam*HI, and inserted into pXY01.

To generate the binary plasmid pXY01-mCherry×4, the mCherry coding sequence with a peptide linker was amplified with the primer pair P1003/P1004, digested with *Xho*I and *Bam*HI, and inserted into pXY01 to obtain pXY01-mCherry first. The mCherry coding sequence was further amplified from the plasmid pXY01-mCherry with the primer pair P1005/P1006, digested with *Xba*I and *Sa*II, and inserted into pXY01-mCherry (digested with *Xba*I and *Xho*I), the procedure was repeated twice more to obtain the binary plasmid pXY01-mCherry×4.

The VirE2(217-243), VirE2(276-306), VirD2(338-356) or SV40 NLS coding sequences were amplified with the primer pairs P1007/P1008, P1009/P1010, P1011/P1012 or P1013/P1014, digested with *Xba*I and *Xho*I, and inserted into pXY01-

mCherry \times 4 to obtain pXY01-VirE2(nls1)-mCherry \times 4, pXY01-VirE2(nls2)-mCherry \times 4, pXY01-VirD2(nlsC1)-mCherry \times 4 or pXY01-SV40(nls)-mCherry \times 4, respectively.

Yeast two-hybrid plasmids

To generate yeast two-hybrid plasmids expressing translational fusions of importin α isoforms to the GAL4 AD, the nine importin α isoforms coding sequences of *A. thaliana* was amplified from an *A. thaliana* cDNA preparation with primer pairs P1015/P1016, P1017/P1018, P1019/P1020, P1021/P1022, P1023/P1024, P1025/P1026, P1027/P1028, P1029/P1030 or P1031/P1032, digested with *Xma*I and *Sal*I, and inserted into pGADT7 (digested with *Xma*I and *Xho*I) to obtain pGADT7-IMP1, pGADT7-IMP2, pGADT7-IMP3, pGADT7-IMP4, pGADT7-IMP5, pGADT7-IMP6, pGADT7-IMP7, pGADT7-IMP8 or pGADT7-IMP9, respectively.

To generate yeast two-hybrid plasmids expressing translational fusions of FG-Nups to the GAL4 AD, the coding sequences of CG1, Nup50A, Nup54, Nup58, Nup62, Nup98A or Nup136 were amplified from an *A. thaliana* cDNA preparation with primer pairs P1033/P1034, P1035/P1036, P1037/P1038, P1039/P1040, P1041/P1042, P1043/P1044 or P1045/P1046, digested with *Xma*I and *Xho*I, and inserted into pGADT7 to obtain pGADT7-CG1, pGADT7-Nup50A, pGADT7-Nup54, pGADT7-Nup58, pGADT7-Nup62, pGADT7-Nup98A or pGADT7-Nup136, respectively. The coding sequences of Nup50B or Nup98B were amplified from an *A. thaliana* cDNA preparation with primer pairs P1047/P1048 or P1049/P1050, digested with *Xma*I and *Sal*I and inserted into pGADT7 (digested with *Xma*I and *Xho*I) to obtain pGADT7-Nup50B or pGADT7-Nup98B, respectively. The coding sequence of Nup214 was amplified from an *A. thaliana* cDNA preparation with the primer pair P1051/P1052, digested with *Nde*I and *Xho*I, and inserted into pGADT7 to obtain pGADT7-Nup214.

To generate yeast two-hybrid plasmids expressing translational fusions of NbCG1A and NbCG1B to the GAL4 AD, the coding sequence of NbCG1A or NbCG1B was amplified from an *N. benthamiana* cDNA preparation with primer pairs P1053/P1054 or P1055/P1056, digested with *Xma*I and *Xho*I and inserted into pGADT7 to obtain pGADT7-CG1A or pGADT7-CG1B, respectively.

To generate yeast two-hybrid plasmids expressing translational fusions of truncated regions of VirE2 to the GAL4 AD, the coding sequences of VirE2(217-306), VirE2(307-549), VirE2(1-216), VirE2(1-99) or VirE2(100-216) were amplified from total DNA of *A. tumefaciens* EHA105 with the primer pairs P1057/P1058, P1059/P1060, P1061/P1062, P1061/P1063 or P1064/P1062, digested with *Nco*I and *Xho*I and inserted into pGBKT7 to obtain pGBKT7-VirE2(217-306), pGBKT7-VirE2(307-549), pGBKT7-VirE2(1-216), pGBKT7-VirE2(1-99) or pGBKT7-VirE2(100-216), respectively. To generate pGBKT7-VirE2(Δ 217-306), the coding sequences of the VirE2 N-terminus and C-terminus were amplified from total DNA of *A. tumefaciens* EHA105 with the primer pairs P1065/P1066 and P1067/P1068. The PCR products were further amplified with the primer pair P1061/P1060 using overlapping PCR, digested with *Nco*I and *Xho*I, and inserted into pGBKT7 (digested with *Nco*I and *Sal*I) to obtain pGBKT7-VirE2(Δ 217-306).

To generate pGBKT7-VirD2, the coding sequence of VirD2 was amplified from total DNA of *A. tumefaciens* strain EHA105 with the primer pair P1069/P1070, digested with *Nco*I and *Xho*I, and inserted into pGBKT7 (digested with *Nco*I and *Sal*I).

In vitro pull-down plasmids

To generate plasmids expressing translational fusions of importin α isoforms to GST, the nine importin α isoforms coding sequences of *A. thaliana* was individually amplified from an *A. thaliana* cDNA preparation with the primer pairs P1015/P1016, P1017/P1018, P1019/P1020, P1021/P1022, P1023/P1024, P1025/P1026, P1027/P1028, P1029/P1030 or P1031/P1032, digested with *Xma*I and *Sal*I, and inserted into pGEX-4T-1 (digested with *Xma*I and *Xho*I) to obtain pGST-IMP1, pGST-IMP2, pGST-IMP3, pGST-IMP4, pGST-IMP5, pGST-IMP6, pGST-IMP7, pGST-IMP8 or pGST-IMP9, respectively.

To generate pGST-VirE3C, the coding sequence of VirE3(596-648) was amplified from total DNA of *A. tumefaciens* EHA105 with the primer pair P1071/P1072, digested with *Bam*HI and *Xho*I and inserted into pGEX-4T-1.

To generate plasmids expressing translational fusions of CG1, NbCG1A and NbCG1B to the MBP, the coding sequence of CG1, NbCG1A or NbCG1B was amplified with the primer pairs P1073/P1034, P1074/P1054 or P1075/P1056, digested with *Bam*HI and *Xho*I, and inserted into pMAL-c2x (digested with *Bam*HI and *Sal*I) to obtain pMBP-CG1, pMBP-NbCG1A or pMBP-NbCG1B, respectively.

To generate pRSET-E2, the VirE2 coding sequence was amplified from total DNA of *A. tumefaciens* EHA105 with the primer pair P1076/P1077, digested with *Xba*I and *Kpn*I, and inserted into pRSET-A. To generate pRSET-D2, the VirD2 coding sequence was amplified from total DNA of *A. tumefaciens* EHA105 with the primer pair P1078/P1079, digested with *Xba*I and *Xho*I, and inserted into pRSET-A.

VIGS plasmids

To generate pTRV2-NbCG1A/NbCG1B, the partial coding sequence of NbCG1B was amplified from an *N. benthamiana* cDNA preparation with the primer pair P1080/P1081, digested with *Xba*I and *Xho*I, and inserted into pTRV2.

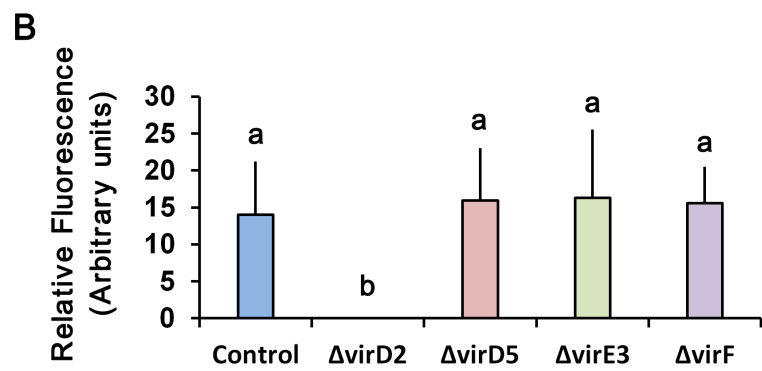
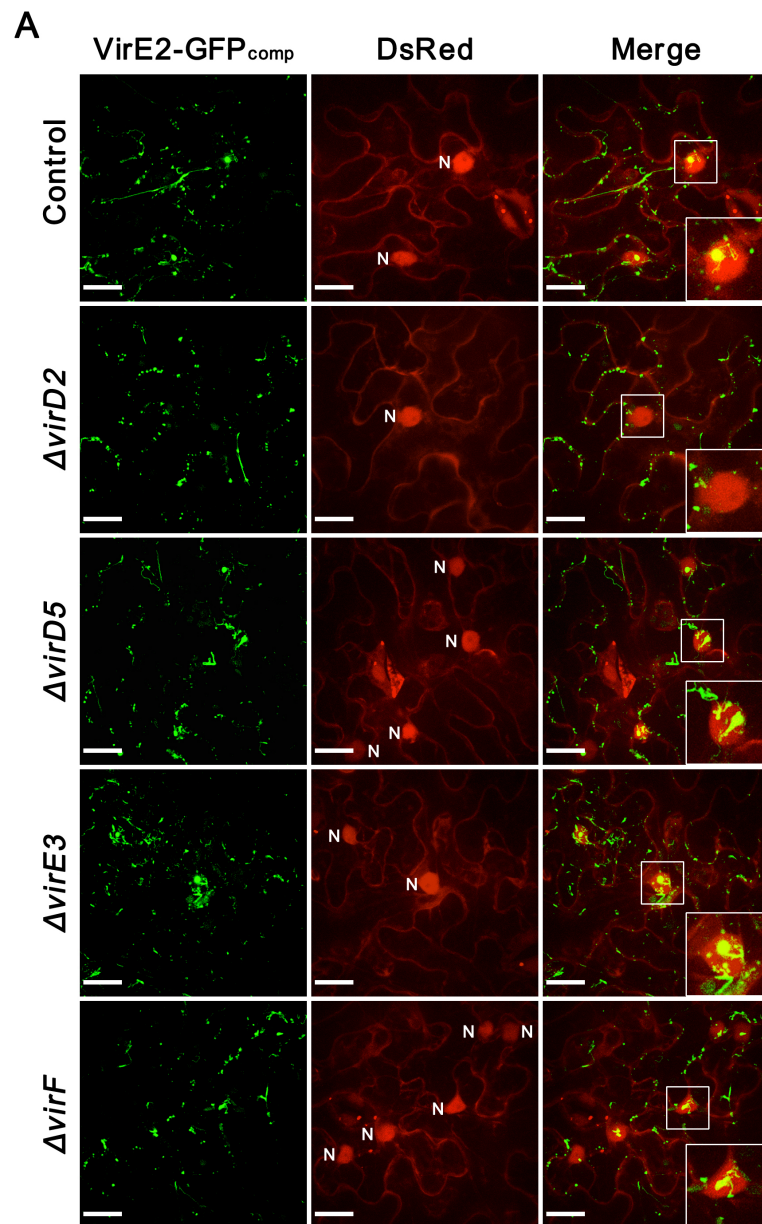


Fig. S1. Localization of *Agrobacterium*-delivered VirE2 from deletion mutants of different effectors. (A) Transgenic *N. benthamiana* (Nb308A) leaves were infiltrated with *A. tumefaciens* strains EHA105virE2::*GFP11* (control), EHA105virE2::*GFP11ΔvirD2*, EHA105virE2::*GFP11ΔvirD5*, EHA105virE2::*GFP11ΔvirE3*, or EHA105virE2::*GFP11ΔvirF*. (B) The fluorescence intensity of VirE2-GFP_{comp} signals was measured in each host nucleus. The data are presented as the means ± SD of n = 30 independent samples. p < 0.01. DsRed expression in *N. benthamiana* leaf epidermal cells facilitated the visualization of the cellular borders and the round/oval nuclei (N). The boxed areas are enlarged to highlight host nuclei. Scale bars, 20 μm.

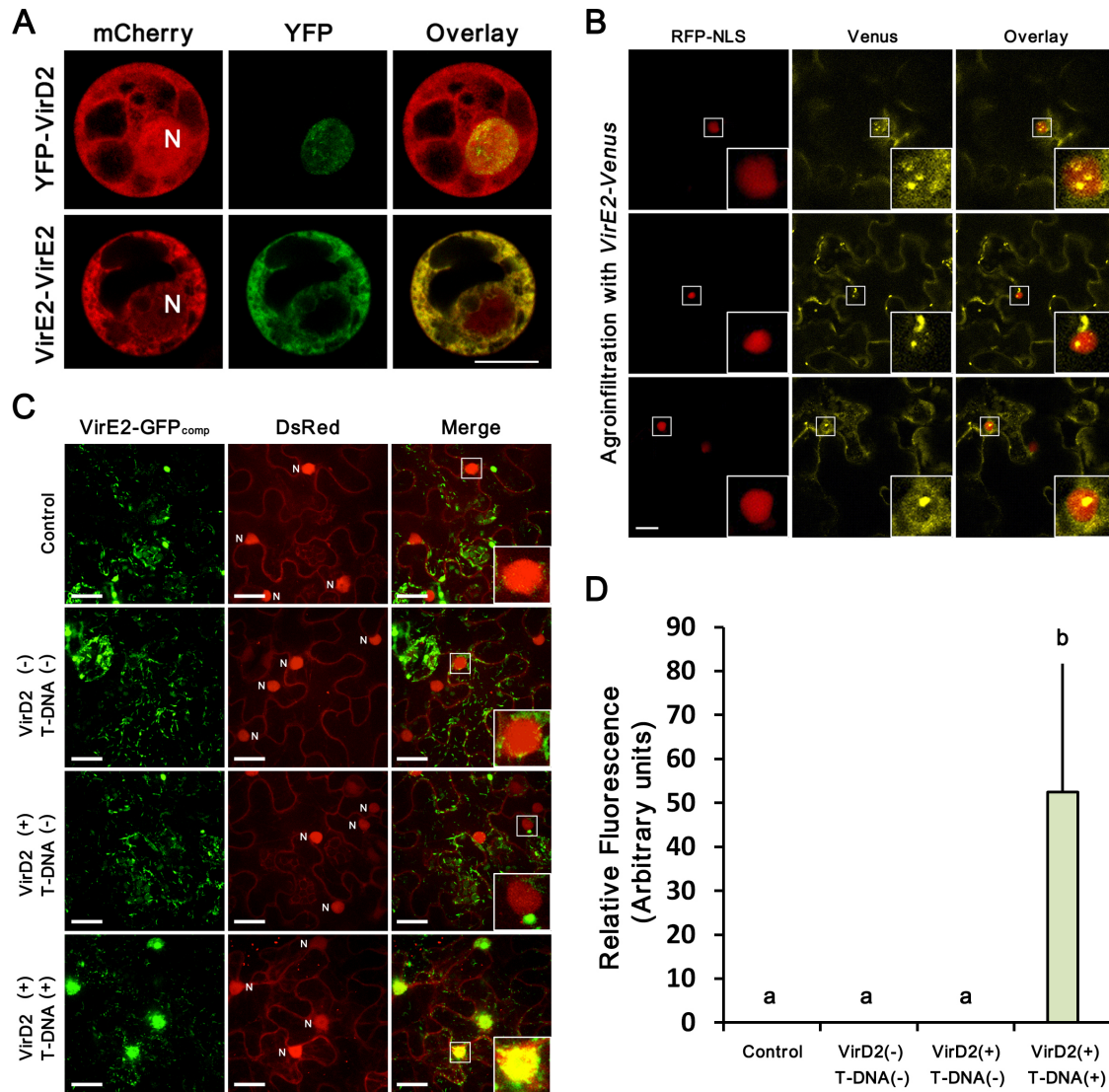


Fig. S2. Subcellular localization of VirD2, VirE2, and VirE2-VirE2 complexes in tobacco cells. (A) Tobacco BY-2 protoplasts were co-electroporated with a construct that expresses mCherry in the nucleus (N) and cytoplasm, and constructs expressing YFP-VirD2 (upper panels) or VirE2-cYFP and VirE2-nYFP (lower panels), as indicated. The cells were imaged by confocal microscopy 18 hours later. (B) *N. benthamiana* leaves were infiltrated with *A. tumefaciens* At2065 containing within the T-DNA region genes expressing an RFP-NLS nuclear marker and VirE2-Venus. The leaves were imaged by confocal microscopy 18 hours later. Three representative fields of cells are shown. The boxed areas are enlarged to highlight host nuclei. (C) Both VirD2 and T-DNA are required for the import of expressed VirE2-GFP_{comp} into the plant nucleus. Transgenic *N. benthamiana* (Nb308E2) (expressing DsRed, GFP1-10 and VirE2-GFP11) leaves were infiltrated with H₂O (Control), *A. tumefaciens* strains XYA105Δ*virD2*Δ*virD5*Δ*virE2*Δ*virE3*Δ*virF* (VirD2-/T-DNA-),

XYA105 Δ *virD5* Δ *virE2* Δ *virE3* Δ *virF* (VirD2+/T-DNA-) or XYA105 Δ *virD5* Δ *virE2* Δ *virE3* Δ *virF* containing a binary plasmid pXY01 (VirD2+/T-DNA+). (D) The fluorescence intensity of VirE2-GFP_{comp} signals was measured in each host nucleus. The data are presented as the means \pm SD of n = 30 independent samples. p < 0.01. DsRed expression in *N. benthamiana* leaf epidermal cells facilitated the visualization of the cellular borders and the round/oval nuclei (N). The boxed areas are enlarged to highlight host nuclei. Scale bars, 20 μ m.

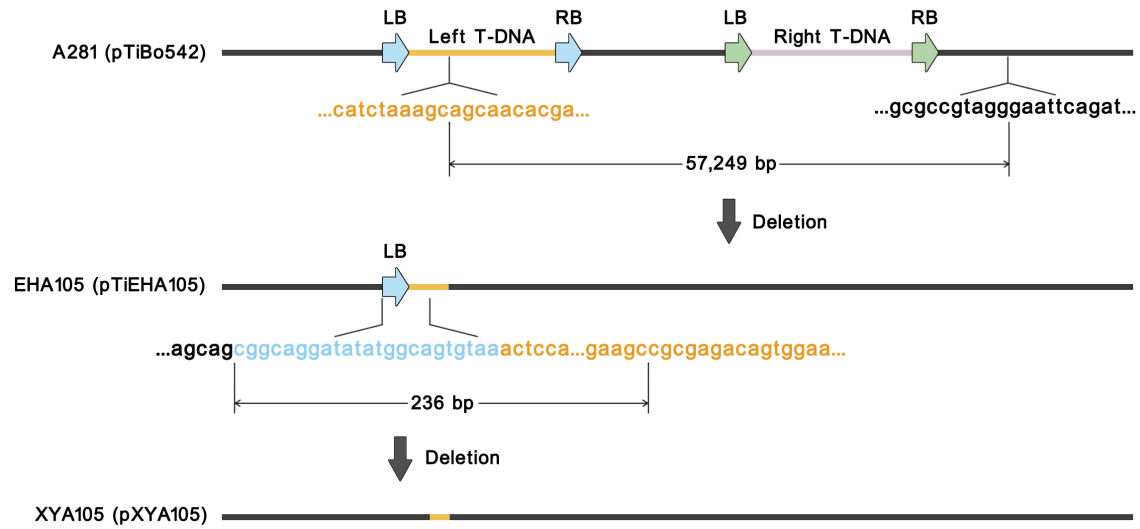


Fig. S3. Schematic representation of the generation of the Ti plasmids pTiEHA105 and pXYA105 from pTiBo542. The Ti plasmid pTiEHA105 was sequentially generated, first by replacement of a fragment containing the majority of the T-DNA region from pTiBo542 with a *nptII* gene to generate pTiEH101, then by deletion of the *nptII* gene as described (2). A 236 bp fragment containing the remaining left border from pTiEHA105 was deleted in this study to generate the Ti plasmid pXYA105, which contains no T-DNA border.

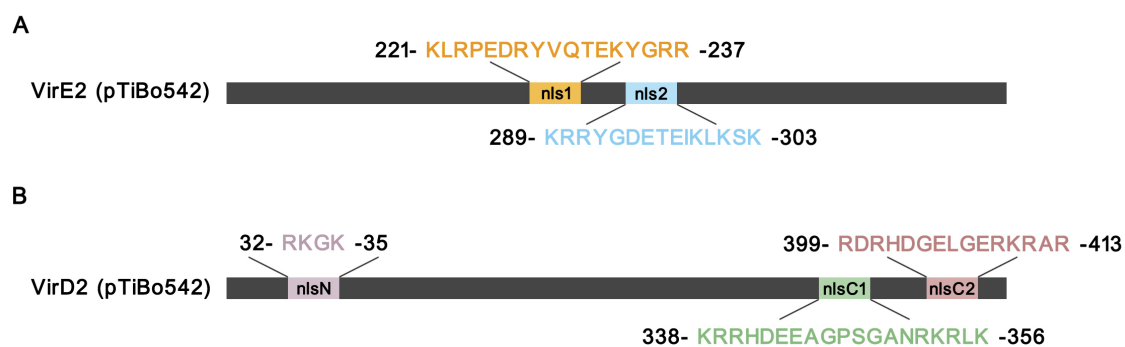


Fig. S4. Schematic representation of the putative NLSs of VirE2 and VirD2. (A) VirE2 contains two putative NLS in the middle of the protein. (B) VirD2 contains a putative NLS at the N-terminus and two putative NLSs at the C-terminus.

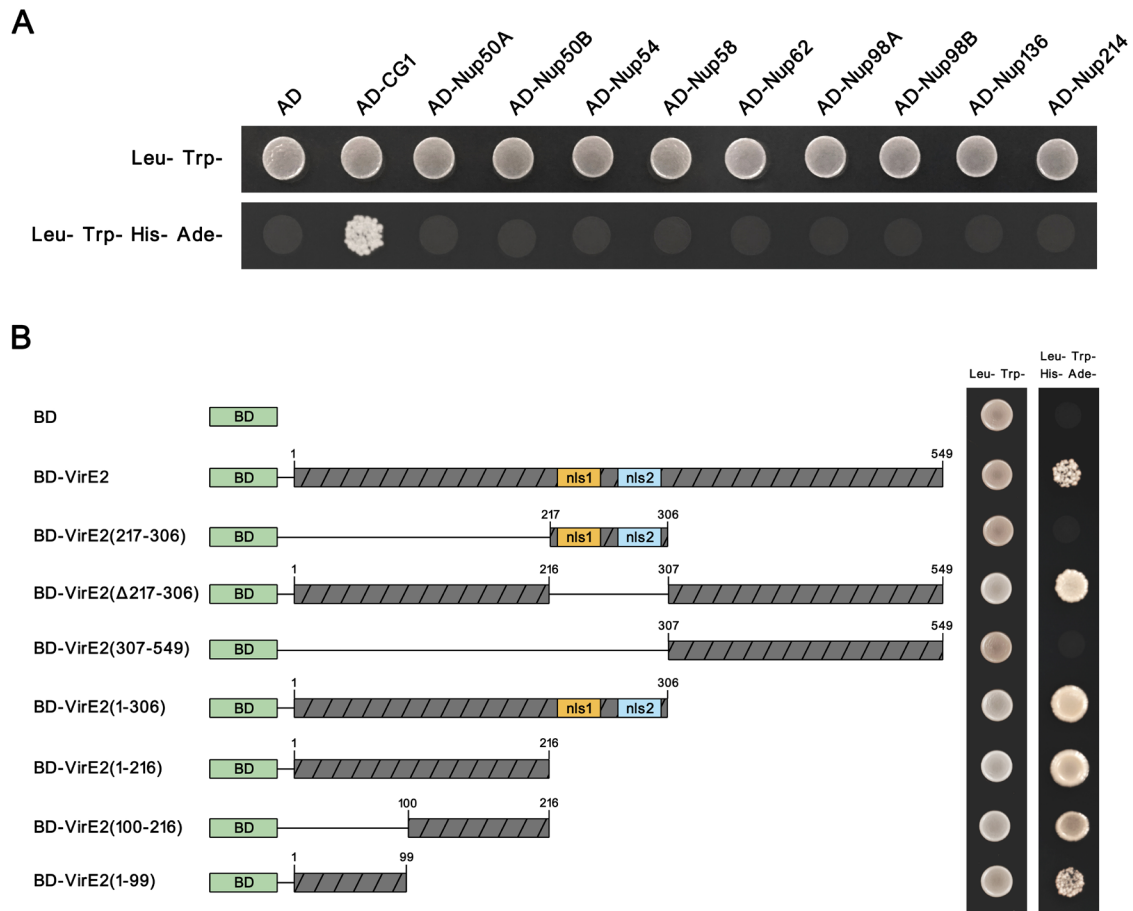


Fig. S5. Yeast two-hybrid assays of VirE2 for interactions with *A. thaliana* FG-Nups. (A) VirE2 interacts with the *A. thaliana* FG-Nup CG1 in the yeast two-hybrid assay. The FG-Nups were expressed as translational fusions to the GAL4 AD and VirE2 was expressed as a translational fusion to the GAL4 BD. (B) VirE2 interacts with *A. thaliana* CG1 through its N-terminal domain. CG1 was expressed as a translational fusion to the GAL4 AD; VirE2 and its truncated constructs were expressed as translational fusions to the GAL4 BD.

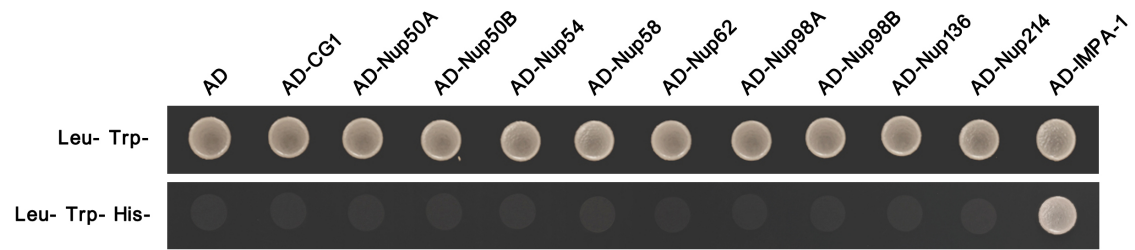


Fig. S6. VirD2 does not interact with *A. thaliana* FG-Nups in yeast two-hybrid assays. The FG-Nups were expressed as translational fusions to the GAL4 AD and VirD2 was expressed as a translational fusion to the GAL4 BD. Interaction of BD-VirD2 with AD-IMPA-1 served as a positive control.

AtCG1 ..MRRELCRNFCRGSCRYGNCFLFP.CCAKPNFEGFCITNQCCQCCQCNSNFGFGVSGGSSSEN.....CFQNTWSRTASFTGGGAARSTCTGKTOTPALEK 104
 NbCG1A MPERRRRCRNFLRGSCCYGDRCKFLAWSQCCPKNFEGFGSCPSNRONTINIOCTRSNMGFGVGNFQPRGSNDLGPCKSPYKAFENKWRSTSTINSSSRCSNDQCPVAPNHT 113
 NbCG1B MPERRRRCRNFLRGSCCYGERCKFLAWQCCPKNFEGFGSCPSNRONTINIOCTRSNMGFGVGNFQPRGSNDLGPCKSQYKAFENKWRSTSTINSSSRCSNDQCPVAPNHT 113
 Consensus rke ctnf rgsc yg c flh qq n fgfg q q qq snp gfgvq x r q t s q q h

 AtCG1 CTDPAACRQVMQIDFENRFRMFLTCYGHFNYFPCDVIGLISYEELRAVAYEDAKRGILFCSIVERERNLNSKLAEFENLRNPKYG...SVIANQSPFAATTPE..SIFGQSS 213
 NbCG1A CTDSDWCRQIMDFENRFRMFLTCYGHFNYFPCDVIGLISYEELRAVAYEDAKRGILFCSIVERERNLNSKLAEFENLRNPKYVFPSTSVENACQSPFPGAAASNLGACSE 226
 NbCG1B CTDSDSFRQIMDFENRFRMFLTCYGHFNYFPCDVIGLISYEELRAVAYEDAKRGILFCSIVERERNLNSKLAEFENLRNPKYVFPSTSVENACQSPFPGAAASNLGACSE 226
 Consensus ctd c r df ne pmw ltcygh k pcdvtgd syeelra ay akrg l siverern nsk aefen lrn sv qspf s qs

 AtCG1 QINSFSEFSGFNQQTAFSNTNAGGLSSSGHFAAFASFNQQTIFPNTNAGGVSSSGFENPFASFQCSSNQQTAFSNTNAGGLSSSGPPNAFASFNKQHNAFSVNTFQVPSG 326
 NbCG1A FPGTAPNALSQAQSPFPGTAPNALSSTGSPFPGAA.....PNASLRACSSFFHSASSHSQLGALLNTGASAPHTNIFQHSPLGNSVKTSSSSRNAFSEFGNAG...SG 327
 NbCG1B FPGTAPNALSQAQSPFPGTAPNALSSTGSPFPGAA.....PNASLRACSSFFHSASSHSQLGALLNTGASAPHTNIFQHSPLGNSVKTSSSSRNAFSEFGNAG...SG 327
 Consensus a na s p a pn ss p s n tn g s s nafs sg

 AtCG1 PSGFCTNPSTTFKFASTGFGPGFTTFCNNIFGCGSTETFA...INISQNNCTAFNFNVEVASFTAPAINITKTSGGTFLQIGGDEVSSINWKEKNGGEIPPCAPPDAFV 435
 NbCG1A SHGFSSQVISQSHQNFETESNISSSERPFSTSQHFENSS...GSQLETFCHRHSSASVAVSPFN...INLTNAATEPFSG.....DINSINWKEKNGGEIPPCAPPDKYI 428
 NbCG1B SHGFSSQVISQSHQNFETESNISSSERPFSTSTTSQHFENSGQLETCGHHSASVAVSEVN...INLTNAATEPFSG.....DINSINWKEKNGGEIPPCAPPDRIYI 430
 Consensus gf f p a n q f v v in tn s e d siw k w geipe appd

Fig. S7. Sequence alignment of *A. thaliana* CG1 and its homologs from *N. benthamiana*. The amino acid sequence of *A. thaliana* CG1 (NCBI accession number: NP_565108.2) was aligned with its *N. benthamiana* homologs NbCG1A (NCBI accession number: BAO49736.1) and NbCG1B (NCBI accession number: BAO49737.1) using the DNAMAN software (Version 7.0.2.176).

NbCG1A ATGCCCCAGGAAAGAACCCGTCAGAAATTTCTGCGTGGCAGCTGTCAATATGGTGA CTTGTGTAATTTCTTCATGTT CCCAACACAGCCGAAGC 100
 NbCG1B ATGCCCCAGGAAAGAACCCGTCAGAAATTTCTGCGTGGCAGCTGTCAATATGGTGA CTTGTGTAATTTCTTCATGTT CCCAACACAGCCGAAGC 100
 Consensus atgcccc aggaagaacccctgcagaaatcttctgctggcagctgtcaatatgggtga cttgtgtaaatcttctcatggt cccaacaacagccgaagc

 NbCG1A CAAATCATTGGGTTTGGCAGCCAGCCCTCTAATTTTCAGAAATACGAATCTGCAGCAGACAAAGTCCAACCCCTATGGTTC GTGTTCAGAACAACTT 200
 NbCG1B CAAATCATTGGGTTTGGCAGCCAGCCCTCTAATTTTCAGAAATACGAATCTGCAGCAGACAAAGTCCAACCCCTATGGTTC GTGTTCAGAACAACTT 200
 Consensus caaat catttggggttggcagccagccctctaattttcagaaatacgaatctgcagcagacaaagtccaacccctatggttt ggtgttcagaaacaactt

 NbCG1A TCAGCCTAGAGGGTCCACGATCTGGGGCCCAACAGAGTC ATATAAGGCTTTCGAAAATAAGTGGACTCGTTCTACAAGTACCAACAGTTCTTCATCG 300
 NbCG1B TCAGCCTAGAGGGTCCACGATCTGGGGCCCAACAGAGTC ATATAAGGCTTTCGAAAATAAGTGGACTCGTTCTACAAGTACCAACAGTTCTTCATCG 300
 Consensus tcagcctagaggggtccacgatctggggcccaaacagagtc atataaggcttttcgaaaataagtggactcgttctacaagtaccaacagttctttcatcg

 NbCG1A CGGCAATCTGACAATCAGCCTGTAGCACCTAATCACACCTGCACAGATTCTGACTG TGCAGACGCCAAATATGGAAGATTTTAATGAGAAGCC TA 400
 NbCG1B CGGCAATCTGACAATCAGCCTGTAGCACCTAATCACACCTGCACAGATTCTGACTG TGCAGACGCCAAATATGGAAGATTTTAATGAGAAGCC TA 400
 Consensus cggcaatctgacaatcagcctgtagcacctaatacacacctgcacagattctgact tgcagacgccaaattatggaagattttaataatgagaagcc a

 NbCG1A TGTGTTTGTACATGCTATGGTCATCGTAAACCGGTCATGTGATGTTAC GGTGATGTTAGCTATGAAGAG TACGAGCAGCAGCATATGATGATGC 500
 NbCG1B TGTGTTTGTACATGCTATGGTCATCGTAAACCGGTCATGTGATGTTAC GGTGATGTTAGCTATGAAGAG TACGAGCAGCAGCATATGATGATGC 500
 Consensus tgtgtttgttacatgctatggtcacgtgtaaaacgggtccatgtgatgttac ggtgatgttagctatgaagag tacgagcagcagcata gatgatgc

 NbCG1A AAAACGTGGACAGCTTGAIGTCTATTGTTGAGAGAGAGGGAACATGCTTAATCTAAAGCAGCTGAATTGAAAATCT TCGCGGAACATATGATCCT 600
 NbCG1B AAAACGTGGACAGCTTGAIGTCTATTGTTGAGAGAGAGGGAACATGCTTAATCTAAAGCAGCTGAATTGAAAATCT TCGCGGAACATATGATCCT 600
 Consensus aaaacgtggaca agcttgatgtctattgttgagagagagaggaacatgcttaattctaaagcagctgaattgaaaatct ttcggaactatgtac t

 NbCG1A CCATCAACTTCTGTTCTTAATGCTCAAAGTCCTTTTCC GGTGCGCG CAAATGCCCTCATTC GTGCTCAAAGTCCTTTTCTGGTACCGCGCCGAATG 700
 NbCG1B CCATCAACTTCTGTTCTTAATGCTCAAAGTCCTTTTCC GGTGCGCG CAAATGCCCTCATTC GTGCTCAAAGTCCTTTTCTGGTACCGCGCCGAATG 700
 Consensus ccatacaacttctgttcttaatgctcaaagtccttttcc ggtgc gcg caaatgacctcattg gtgctcaaagtccttttctgttacccgcccgaatg

 NbCG1A CCTCATTTAGTGTCAAAGTCCTTTTCTGGTACAGCGCGCAATGCCCTCATTTAGTACTCAAAGTCCTTTTCTGGTGCCGCAACCAATGCATCGTTGAG 800
 NbCG1B CCTCATTTAGTGTCAAAGTCCTTTTCTGGTACAGCGCGCAATGCCCTCATTTAGTACTCAAAGTCCTTTTCTGGTGCCGCAACCAATGCATCGTTGAG 800
 Consensus cctcatttagtgtctcaaagtccttttctgggtacagcgccgaatgccctcattgagtactcaaagtccttttctggtgccgcaccaaatgcacgttgag

 NbCG1A AGCTCAAAGCAGTTTCTCTCTTCAGCCTCAAGTTTTAGTCAGTTGGGAGCTTTACTGAATACAGGGGCATCTGCTCCACCACTAATACATTGGGCAA 900
 NbCG1B AGCTCAAAGCAGTTTCTCTCTTCAGCCTCAAGTTTTAGTCAGTTGGGAGCTTTACTGAATACAGGGGCATCTGCTCCACCACTAATACATTGGGCAA 900
 Consensus agctcaaagcagtttctctcttcagcctcaagtttttagtcagttgggagctttactgaatacaggggcacatctgctccaccaactaatacatattgggcaa

 NbCG1A CCCAGTCCCCCT GGGAACTCTGTTAAGACATCAAGTTCTTCT GGGCGAATGCTTTTTCATTGGGAATGCAGGTTGAGTTCCCTTTGGCTTCGGAAGCC 1000
 NbCG1B CCCAGTCCCCCT GGGAACTCTGTTAAGACATCAAGTTCTTCT GGGCGAATGCTTTTTCATTGGGAATGCAGGTTGAGTTCCCTTTGGCTTCGGAAGCC 1000
 Consensus cccagtcacctt gggaaactctgttaagacatcaagttcttct gggcgaatgctttttcatttgggaatgcaggttcaggttcctttggttcggaaagcc

 NbCG1A AAGTCACATCCCACTCAGATCAAAATCCTTTCACTCC AGCAATATTTTCAGCAAGTCTGAGAGGAAC CATTTT CTACCTCTCAACATT 1091
 NbCG1B AAGTCACATCCCACTCAGATCAAAATCCTTTCACTCC AGCAATATTTTCAGCAAGTCTGAGAGGAAC CATTTT CTACCTCGA CTACCTCTCAACATT 1100
 Consensus aagtcacatcccaactcagatcaaaaatcctttcactcc agcaatattttcagcaagttctgagaggaac catttt ctacctctcaacattt

 NbCG1A TCCTAATTCCTTGGCGGCCAACTTCCTCTCTCAGAGGCAATTTTCTGCTTCAGTTT CGGTGTCCCTT TCAACATCAACTTGACGAATGCTGCATCA 1191
 NbCG1B TCCTAATTCCTTGGCGGCCAACTTCCTCTCTCAGAGGCAATTTTCTGCTTCAGTTT CGGTGTCCCTT TCAACATCAACTTGACGAATGCTGCATCA 1197
 Consensus tctctaatttccttggcgcccaacttcctctctcagagggcaattttctgcttcagttt cgggtgtccctt tcaacatcaacttgacgaatgctgcatca

 NbCG1A ACAGAGGAATTACAGTGGGGATAACAGCATTGGAACAAGGAAGGAATGGAATAATTGGGGAGATTCCAGAAGC AGCACC CCAGACA ATATATCTTTTA 1289
 NbCG1B ACAGAGGAATTACAGTGGGGATAACAGCATTGGAACAAGGAAGGAATGGAATAATTGGGGAGATTCCAGAAGC AGCACC CCAGACA ATATATCTTTTA 1295
 Consensus acagaggaattacagtggggataacagcatttggacaagaaggaatggaaaattggggagattccagaag agcacc ccagaca atatatctttta

Fig. S8. Sequence alignment of *NbCG1A* (NCBI accession number: AB898774.1) and *NbCG1B* (NCBI accession number: AB898775.1) using the DNAMAN software (Version 7.0.2.176). Nucleotide sequence highlighted in green was used for the TRV-based VIGS construct.

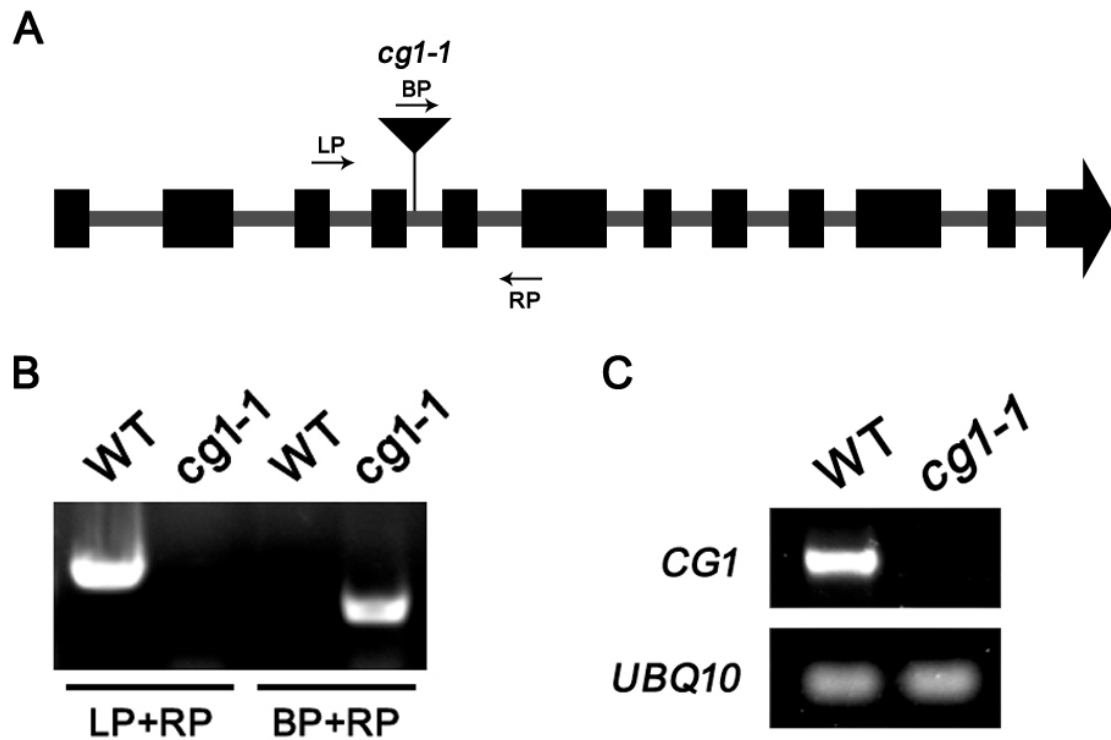


Fig. S9. Identification of a T-DNA insertional line of *A. thaliana CG1*. (A) Schematic representation of the T-DNA insertion at the *CG1* gene. LP, left genomic primer; RP, right genomic primer; BP, left T-DNA border primer. (B) Identification of the *cgl-1* mutant line. Total genomic DNA from the wild-type and *cgl-1* mutant lines was prepared and used for PCR with the indicated primers. (C) RT-PCR analysis of *CG1* transcripts. Total RNA was prepared from the wild-type and *cgl-1* mutant lines followed by first-strand cDNA synthesis. The expression of *CG1* and an endogenous *UBQ10* (control) genes was examined with the primer pairs RT1005/RT1006 and RT1007/RT1008, respectively.

Table S1. *A. tumefaciens* Strains used in this study

<i>A. tumefaciens</i> Strains	Relevant characteristics	Source
EHA105	C58 strain containing pTiBo542 without oncogenic T-DNA region	(2)
EHA105 <i>virE2::GFP11</i>	EHA105 derivative, with the GFP11-coding sequence inserted into <i>virE2</i> on pTiBo542	(3)
EHA105 <i>virE2::GFP11</i> Δ <i>virD2</i>	EHA105 <i>virE2::GFP11</i> derivative, with <i>virD2</i> deleted from the Ti plasmid	This Study
EHA105 <i>virE2::GFP11</i> Δ <i>virD5</i>	EHA105 <i>virE2::GFP11</i> derivative, with <i>virD5</i> deleted from the Ti plasmid	This Study
EHA105 <i>virE2::GFP11</i> Δ <i>virE3</i>	EHA105 <i>virE2::GFP11</i> derivative, with <i>virE3</i> deleted from the Ti plasmid	(4)
EHA105 <i>virE2::GFP11</i> Δ <i>virF</i>	EHA105 <i>virE2::GFP11</i> derivative, with <i>virF</i> deleted from the Ti plasmid	This Study
XYA105	EHA105 derivative, with the T-DNA left border deleted from the Ti plasmid	This Study
XYA105 <i>virE2::GFP11</i>	EHA105 <i>virE2::GFP11</i> derivative, with the T-DNA left border deleted from the Ti plasmid	This Study
XYA105Δ <i>virD5</i> Δ <i>virE2</i> Δ <i>virE3</i> Δ <i>virF</i>	XYA105 derivative, with <i>virD5</i> , <i>virE2</i> , <i>virE3</i> and <i>virF</i> deleted from the Ti plasmid	This study
XYA105Δ <i>virD2</i> Δ <i>virD5</i> Δ <i>virE2</i> Δ <i>virE3</i> Δ <i>virF</i>	XYA105 derivative, with <i>virD2</i> , <i>virD5</i> , <i>virE2</i> , <i>virE3</i> and <i>virF</i> deleted from the Ti plasmid	This study

A348	A136 (pTiA6NC) (Octopine-type)	(5)
GV3101(pMP90)	C58 strain containing pMP90 without T-DNA	(6)
At2065	GV3101(pMP90) containing within the T- DNA region P _{nos} -VirE2- Venus and P _{35S} -RFP- NLS genes	(7)

Table S2. Plasmids used in this study

Plasmids	Relevant characteristics	Source
pXY01	A binary plasmid for target gene expression under the control of CaMV 35S promoter; Km ^r	(8)
pXY01-GFP	pXY01 derivative, with the GFP coding sequence placed downstream of the CaMV 35S promoter; Km ^r	This Study
pXY01-mCherry _{×4}	pXY01 derivative, with tandem 4× mCherry coding sequence placed downstream of the CaMV 35S promoter; Km ^r	This Study
pXY01-VirE2(nls1)-mCherry _{×4}	pXY01-mCherry _{×4} derivative, with VirE2(217-243) coding sequence fused to the N-terminus of mCherry _{×4} ; Km ^r	This Study
pXY01-VirE2(nls2)-mCherry _{×4}	pXY01-mCherry _{×4} derivative, with VirE2(276-306) coding sequence fused to the N-terminus of mCherry _{×4} ; Km ^r	This Study
pXY01-VirD2(nlsC1)-mCherry _{×4}	pXY01-mCherry _{×4} derivative, with VirD2(338-356) coding sequence fused to the N-terminus of mCherry _{×4} ; Km ^r	This Study
pXY01-SV40(nls)-mCherry _{×4}	pXY01-mCherry _{×4} derivative, with SV40 NLS coding sequence fused to the N-terminus of mCherry _{×4} ; Km ^r	This Study
pEx18Km	Counter-selectable plasmid carrying <i>sacB</i> marker; Km ^r	(3)
pEx18Km-ΔVirD2	pEx18Km derivative, to delete the sequence encoding VirD2 on pTiBo542; Km ^r	(4)
pEx18Km-ΔVirD5	pEx18Km derivative, to delete the sequence encoding VirD5 on pTiBo542; Km ^r	(4)
pEx18Km-ΔVirE2	pEx18Km derivative, to delete the sequence encoding VirE2 on pTiBo542; Km ^r	(3)
pEx18Km-ΔVirE3	pEx18Km derivative, to delete the sequence encoding VirE3 on pTiBo542; Km ^r	(4)

pEx18Km-ΔVirF	pEx18Km derivative, to delete the sequence encoding VirF on pTiBo542; Km ^r	(4)
pEx18Km-ΔLB	pEx18Km derivative, to delete the T-DNA left border sequence on pEHA105; Km ^r	This Study
pGADT7	Yeast two-hybrid cloning plasmid, with the GAL4 AD domain; Amp ^r	Clontech
pGADT7-IMPA1	pGADT7 derivative, with the IMPA1 coding sequence fused to the GAL4 AD domain; Amp ^r	This Study
pGADT7-IMPA2	pGADT7 derivative, with the IMPA2 coding sequence fused to the GAL4 AD domain; Amp ^r	This Study
pGADT7-IMPA3	pGADT7 derivative, with the IMPA3 coding sequence fused to the GAL4 AD domain; Amp ^r	This Study
pGADT7-IMPA4	pGADT7 derivative, with the IMPA4 coding sequence fused to the GAL4 AD domain; Amp ^r	This Study
pGADT7-IMPA5	pGADT7 derivative, with the IMPA5 coding sequence fused to the GAL4 AD domain; Amp ^r	This Study
pGADT7-IMPA6	pGADT7 derivative, with the IMPA6 coding sequence fused to the GAL4 AD domain; Amp ^r	This Study
pGADT7-IMPA7	pGADT7 derivative, with the IMPA7 coding sequence fused to the GAL4 AD domain; Amp ^r	This Study
pGADT7-IMPA8	pGADT7 derivative, with the IMPA8 coding sequence fused to the GAL4 AD domain; Amp ^r	This Study
pGADT7-IMPA9	pGADT7 derivative, with the IMPA9 coding sequence fused to the GAL4 AD domain; Amp ^r	This Study
pGADT7-VirE3	pGADT7 derivative, with the VirE3 coding sequence fused to the GAL4 AD domain; Amp ^r	(4)
pGADT7-CG1	pGADT7 derivative, with the CG1 coding sequence fused to the GAL4 AD domain; Amp ^r	This Study
pGADT7-Nup50A	pGADT7 derivative, with the Nup50A coding sequence fused to the GAL4 AD domain; Amp ^r	This Study

pGADT7-Nup50B	pGADT7 derivative, with the Nup50B coding sequence fused to the GAL4 AD domain; Amp ^r	This Study
pGADT7-Nup54	pGADT7 derivative, with the Nup54 coding sequence fused to the GAL4 AD domain; Amp ^r	This Study
pGADT7-Nup58	pGADT7 derivative, with the Nup58 coding sequence fused to the GAL4 AD domain; Amp ^r	This Study
pGADT7-Nup62	pGADT7 derivative, with the Nup62 coding sequence fused to the GAL4 AD domain; Amp ^r	This Study
pGADT7-Nup98A	pGADT7 derivative, with the Nup98A coding sequence fused to the GAL4 AD domain; Amp ^r	This Study
pGADT7-Nup98B	pGADT7 derivative, with the Nup98B coding sequence fused to the GAL4 AD domain; Amp ^r	This Study
pGADT7-Nup136	pGADT7 derivative, with the Nup136 coding sequence fused to the GAL4 AD domain; Amp ^r	This Study
pGADT7-Nup214	pGADT7 derivative, with the Nup214 coding sequence fused to the GAL4 AD domain; Amp ^r	This Study
pGADT7-NbCG1A	pGADT7 derivative, with the NbCG1A coding sequence fused to the GAL4 AD domain; Amp ^r	This Study
pGADT7-NbCG1B	pGADT7 derivative, with the NbCG1B coding sequence fused to the GAL4 AD domain; Amp ^r	This Study
pGBKT7	Yeast two-hybrid cloning plasmid, with the GAL4 BD domain; Km ^r	Clontech
pGBKT7-VirE2	pGBKT7 derivative, with the VirE2 coding sequence fused to the GAL4 BD domain; Km ^r	(4)
pGBKT7-VirE2(217-306)	pGBKT7 derivative, with the VirE2(217-306) coding sequence fused to the GAL4 BD domain; Km ^r	This Study
pGBKT7-VirE2(Δ 217-306)	pGBKT7 derivative, with the VirE2(Δ 217-306) coding sequence fused to the GAL4 BD domain; Km ^r	This Study
pGBKT7-VirE2(307-549)	pGBKT7 derivative, with the VirE2(307-549) coding sequence fused to the GAL4 BD domain; Km ^r	This Study

pGBKT7-VirE2(1-216)	pGBKT7 derivative, with the VirE2(1-216) coding sequence fused to the GAL4 BD domain; Km ^r	This Study
pGBKT7-VirE2(1-99)	pGBKT7 derivative, with the VirE2(1-99) coding sequence fused to the GAL4 BD domain; Km ^r	This Study
pGBKT7-VirE2(100-216)	pGBKT7 derivative, with the VirE2(100-216) coding sequence fused to the GAL4 BD domain; Km ^r	This Study
pGBKT7-VirD2	pGBKT7 derivative, with the VirD2 coding sequence fused to the GAL4 BD domain; Km ^r	This Study
pGEX-4T-1	GST tag expression vector; Amp ^r	GE Healthcare
pGST-IMPA1	pGEX-4T-1 derivative, with the IMPA1 coding sequence fused to the GST coding sequence; Amp ^r	This Study
pGST-IMPA2	pGEX-4T-1 derivative, with the IMPA2 coding sequence fused to the GST coding sequence; Amp ^r	This Study
pGST-IMPA3	pGEX-4T-1 derivative, with the IMPA3 coding sequence fused to the GST coding sequence; Amp ^r	This Study
pGST-IMPA4	pGEX-4T-1 derivative, with the IMPA4 coding sequence fused to the GST coding sequence; Amp ^r	This Study
pGST-IMPA5	pGEX-4T-1 derivative, with the IMPA5 coding sequence fused to the GST coding sequence; Amp ^r	This Study
pGST-IMPA6	pGEX-4T-1 derivative, with the IMPA6 coding sequence fused to the GST coding sequence; Amp ^r	This Study
pGST-IMPA7	pGEX-4T-1 derivative, with the IMPA7 coding sequence fused to the GST coding sequence; Amp ^r	This Study
pGST-IMPA8	pGEX-4T-1 derivative, with the IMPA8 coding sequence fused to the GST coding sequence; Amp ^r	This Study
pGST-IMPA9	pGEX-4T-1 derivative, with the IMPA9 coding sequence fused to the GST coding sequence; Amp ^r	This Study
pGST-VirE3C	pGEX-4T-1 derivative, with the VirE3(596-648) coding sequence	This Study

	fused to the GST coding sequence; Amp ^r	
pMAL-c2x	MBP tag expression vector; Amp ^r	New England Biolabs
pMBP-CG1	pMAL-c2x derivative, with the CG1 coding sequence fused to the MBP coding sequence; Amp ^r	This Study
pMBP-NbCG1A	pMAL-c2x derivative, with the NbCG1A coding sequence fused to the MBP coding sequence; Amp ^r	This Study
pMBP-NbCG1B	pMAL-c2x derivative, with the NbCG1B coding sequence fused to the MBP coding sequence; Amp ^r	This Study
pRSET-A	Protein expression vector; Amp ^r	Invitrogen
pRSET-E2	pRSET-A derivative, with the VirE2 coding sequence placed downstream of the T7 promoter; Amp ^r	This Study
pRSET-D2	pRSET-A derivative, with the VirD2 coding sequence placed downstream of the T7 promoter; Amp ^r	This Study
pTRV1	VIGS vector containing cDNA clone of tobacco rattle virus (TRV) RNA1; Km ^r	(9)
pTRV2	VIGS vector containing cDNA clone of tobacco rattle virus (TRV) RNA2; Km ^r	(9)
pTRV2-NbCG1A/NbCG1B	pTRV2 derivative, to target transcripts of <i>NbCG1A</i> and <i>NbCG1B</i> in VIGS; Km ^r	This Study

Table S3. Primers used in this study

Primers	Sequences (5' to 3')
E1001	TTCGCAGGCTCGGACAAG
E1002	TTCCACTGTCCTGCTGCAGAGGTGCGGTA
E1003	TCTGCAGCAGGACAGTGGAATGACCCGTAAG
E1004	GGACGACCAGTCATCATACGC
E1005	CTAGTCTAGATCTTTATCACCGCGCTTTGC
E1006	CCGCTCGAGCGCGAGATCGAGAACGGTAAG
P1001	CCGCTCGAGATGTCTAAAGGTGAAGAATTATTTCACTG
P1002	CGCGGATCCTTATTTGTACAATTCATCCATACCATG
P1003	CCGCTCGAGGGAGGTGGCTCTGGCGGGGGATCAATGGTGAGCAA GGGCGAGGA
P1004	CGCGGATCCTTACTTGTACAGCTCGTCCATGCCG
P1005	CACTATCCTTCGCAAGACCCT
P1006	ACGCGTCGACCTTGTACAGCTCGTCCATGCCG
P1007	GCTCTAGAATGGACCGGAATTATAAACTAAGACCTGA
P1008	CCGCTCGAGATATCGCTTTTGAATTTCCCG
P1009	GCTCTAGAATGTACGCCAACAAACAGTTCAGC
P1010	CCGCTCGAGAATGCCTGACTTTGACTTCAATTT
P1011	GCTCTAGAATGAAACGACGTCATGACGAGGAG
P1012	CCGCTCGAGCTTCAATCTTTTACGGTTTGCTC
P1013	GCTCTAGAATGCCAAAAAAGAAGAGAAAGGT
P1014	CCGCTCGAGGGGGTCTTCTACCTTTCTCTTCT
P1015	TCCCCCGGGAATGTCACTGAGACCCAACGCTA
P1016	ACGCGTCGACTCAGCTGAAGTTGAATCCTCCG
P1017	TCCCCCGGGAATGTCTTTGAGACCTAACGCTAAGA
P1018	ACGCGTCGACTCACTGGAAGTTGAATCCACCTG
P1019	TCCCCCGGGAATGTCTCTCAGACCTAGCGCG
P1020	ACGCGTCGACTCAAATAAAGTTGAATTGACCAGGAG
P1021	TCCCCCGGGAATGTGCTGAGGCCGAGC
P1022	ACGCGTCGACTCAGGCAAATTTGAATCCACC
P1023	TCCCCCGGGAATGTCCTTGCGACCGAGCA
P1024	ACGCGTCGACTTAACGAGAAAAATCAAACCTGGAAT
P1025	TCCCCCGGGAATGTCTTACAAACCAAGCGCG
P1026	ACGCGTCGACTCAACCAAAGTTGAATCCACCC
P1027	TCCCCCGGGAATGAAGGGAGGAGACAATGTC
P1028	ACGCGTCGACTTAAGGTCCGCAGTGCATCTC
P1029	TCCCCCGGGAATGGCTTGGAACACAGAGGTG
P1030	ACGCGTCGACTCACACCTGAAAGTCCACATCAT
P1031	TCCCCCGGGAATGGCGGATGATGGCTCC
P1032	ACGCGTCGACTCATTTCATCGATTCCATAATCTTCA
P1033	TCCCCCGGGAATGAGGAAGGAAGTGTGTAGAACTT

P1034	CCGCTCGAGTTAAACAAAGGCATCAGGCG
P1035	TCCCCCGGGAATGGGTGACTCGGAAAACGTT
P1036	CCGCTCGAGTCAAGTATCTGTAGCTGTTGGAGAGTT
P1037	TCCCCCGGGAATGTTTCGGCACTCCGTCTTC
P1038	CCGCTCGAGCTATGAGTCTAGTGCCATTTCTGTATCT
P1039	TCCCCCGGGAATGTCGTTTTTTCCCCCACA
P1040	CCGCTCGAGCTAACGGCGTGTAGTTCGAGAT
P1041	TCCCCCGGGAATGTCGGGGTTTCCATTG
P1042	CCGCTCGAGTCAAGACATCCAGTGCTTTGGAG
P1043	TCCCCCGGGAATGTTTGGCTCATCTAATCCTTTTG
P1044	CCGCTCGAGCTAAACTCCATCTTCTTCATCTTCGTC
P1045	TCCCCCGGGAATGGCGAGCGCGGCA
P1046	CCGCTCGAGTTATTTCTTCCTGGTGGATTCTTT
P1047	TCCCCCGGGAATGGGGGACTCCGATAATGC
P1048	ACGCGTCGACTCAAGCATCTTCAGCACTCGG
P1049	TCCCCCGGGAATGTTTCGGTTCTTCTAATAATAATCCTT
P1050	ACGCGTCGACCTACACATCATATTCATCTCCAAGCT
P1051	GGAATTCCATATGATGAGCAGAGTTGAGATTGAAGAAG
P1052	CCGCTCGAGTCATTTTCTCATCTGTGTGAAGAGTT
P1053	TCCCCCGGGAATGCCCCCTAGGAAAGAACC
P1054	CCGCTCGAGCTAAAAGATATATTTGTCTGGGGGTG
P1055	TCCCCCGGGAATGCCCCCGAGGAAAGAACC
P1056	CCGCTCGAGCTAAAAGATATATCTGTCTGGTGGTGCTTC
P1057	CATGCCATGGCAGACCGGAATTATAAACTAAGACCTGA
P1058	CCGCTCGAGTTAAATGCCTGACTTTGACTTCAATTT
P1059	CATGCCATGGCAATGCATGACTCGAAATATCTGGA
P1060	CCGCTCGAGTCAAAAGCTGTTGACGCTTTG
P1061	CATGCCATGGATCCGTCTAGCAATGAGAA
P1062	CCGCTCGAGTTAGAGCTTTATGTTCTTATCTGTTTGATAA
P1063	CCGCTCGAGTTAAGACATGTTTCGAGAACAAGACGG
P1064	CATGCCATGGCATTGCCAGGCAACGATCGG
P1065	CGGGTTGCGGAGGATTTTC
P1066	GAGTCATGCATGAGCTTTATGTTCTTATCTGTTTGATAA
P1067	ACATAAAGCTCATGCATGACTCGAAATATCTGGA
P1068	GCGCCTCTTCTTCGGTAATCA
P1069	CATGCCATGGCAATGCCCGATCGCGCTC
P1070	CCGCTCGAGCTAGGTCCCCCGCGC
P1071	CGCGGATCCGGGTTTATTGACCCGCAATC
P1072	CCGCTCGAGTTACGGTGAAGGAACCGGCAG
P1073	CGCGGATCCATGAGGAAGGAAGTGTGTAGAACTT
P1074	CGCGGATCCATGCCCCCTAGGAAAGAACC
P1075	CGCGGATCCATGCCCCCGAGGAAAGAACC

P1076	CTAGTCTAGAAATAATTTTGTTTAACTTTAAGAAGGAGATATACA TATGGATCCGTCTAGCAATGAG
P1077	CGGGGTACCTCAAAAGCTGTTGACGCTTTG
P1078	CTAGTCTAGAAATAATTTTGTTTAACTTTAAGAAGGAGATATACA TATGCCCCGATCGCGCTC
P1079	CCGCTCGAGCTAGGTCCCCCGCGC
P1080	GCTCTAGAGTGCTCAAAGTCCTTTTCCTGG
P1081	CCGCTCGAGGTGAAAGGATTTTGATGTGACTGG
RT1001	CGTGGCAGCTGTCAATATGGT
RT1002	TTCTGAAAATTAGAGGGGCTGGC
RT1003	CTTGAAACAGCAAAGACCAGC
RT1004	GGAATCTCTCAGCACCAATGG
RT1005	ATGAGGAAGGAACTGTGTAGAAACTT
RT1006	TTAAACAAAGGCATCAGGCG
RT1007	GGCCTTGTATAATCCCTGATGAATAAG
RT1008	AAAGAGATAACAGGAACGGAAACATAGT
LP	TAAAGCCAGAGAATGCTGGAG
RP	TTTGTGCTGTTTTTGCAGTTG
BP	GCCTTTTCAGAAATGGATAAATAGCCTTGCTTCC

SI References

1. Hoang TT, Karkhoff-Schweizer RR, Kutchma AJ, & Schweizer HP (1998) A broad-host-range Flp-FRT recombination system for site-specific excision of chromosomally-located DNA sequences: application for isolation of unmarked *Pseudomonas aeruginosa* mutants. *Gene* 212(1):77-86.
2. Hood EE, Gelvin SB, Melchers LS, & Hoekema A (1993) New *Agrobacterium* helper plasmids for gene transfer to plants. *Transgenic Res.* 2(4):208-218.
3. Li X, Yang Q, Tu H, Lim Z, & Pan SQ (2014) Direct visualization of *Agrobacterium*-delivered VirE2 in recipient cells. *Plant J.* 77(3):487-495.
4. Li X, Tu H, & Pan SQ (2018) *Agrobacterium* delivers anchorage protein VirE3 for companion VirE2 to aggregate at host entry sites for T-DNA protection. *Cell reports* 25(2):302-311 e306.
5. Knauf VC & Nester EW (1982) Wide host range cloning vectors: a cosmid clone bank of an *Agrobacterium* Ti plasmid. *Plasmid* 8(1):45-54.
6. Koncz C & Schell J (1986) The promoter of TL-DNA gene 5 controls the tissue-specific expression of chimaeric genes carried by a novel type of *Agrobacterium* binary vector. *Molecular and General Genetics MGG* 204(3):383-396.
7. Shi Y, Lee LY, & Gelvin SB (2014) Is VIP1 important for *Agrobacterium*-mediated transformation? *Plant J.* 79(5):848-860.
8. Li X & Pan SQ (2017) *Agrobacterium* delivers VirE2 protein into host cells via clathrin-mediated endocytosis. *Science advances* 3(3):e1601528.
9. Liu Y, Schiff M, Marathe R, & Dinesh-Kumar SP (2002) Tobacco *Rar1*, *EDS1* and *NPR1/NIM1* like genes are required for N-mediated resistance to tobacco mosaic virus. *Plant J.* 30(4):415-429.